SEABED LOGGING

PROCESSING REPORT

WOLSELEY

SORELL BASIN

OCTOBER 2007

SANTOS LTD

ELECTROMAGNETIC GEOSERVICES AS

ELECTROMAGNETIC GEOSERVICES AS

Stiklestadvn 1
N-7041 Trondheim
Norway

Phone: (+47) 73568810
Fax: (+47) 73568811

www.emgs.com

Processing Report

Wolseley

Author
Naim Abd Rahman

Client
Santos Ltd

C O N F I D E N T I A L

Date: 16.10.2007

Project Manager
Naim Abd Rahman

Reviewed
Stein Fanavoll

Summary

A SeaBed Logging (SBL) survey was performed in Sorell Basin, Australia. The data was acquired in August 2007. A total of 44 receivers were deployed along two lines. All receivers measured both the electric and magnetic field in two orthogonal directions (Ex, Ey, Hx and Hy) with redundant measurements for the electric field. Water depth in the survey area varies from 1700 to 2500 meters.

High quality electric data was recorded up to 8-10 km at 0.25 Hz (base frequency), 8-9 km at 0.50 Hz (second harmonic) and 6.5-7.5 km at 0.75 Hz (third harmonic). The quality of the electric field measurement is slightly higher than the magnetic field measurement. Due to the large water depth in the survey area, no up-down separation of standard processed signals was performed.

At short offsets, weak anomalies are observed close to the crossing point of Wolse01Tx01 and Wolse02Tx01. At large offsets, weak to moderate anomalies are open at both ends for the two lines. Anomalies are indicated by a positive normalized magnitude and negative phase difference. At higher frequencies, noise influences at shorter offsets.

Further analysis should be carried up to understand and explain the data

Keywords, English
SeaBed Logging (SBL) measurements
Processing

Keywords, Norwegian
SeaBed Logging (SBL) målinger
Prosessering av måledata

Table of Contents

1 Introduction 2

2 SBL method 3

2.1 Subsurface resistivities 3

2.2 Transmission of electromagnetic energy 4

3 Data processing methodology and procedures 6

3.1 Standard processing 6

3.2 Up-Down separation 9

3.3 Data Processing Sequence 11

4 Data presentation 12

4.1 Receiver response 12

4.2 Line response 14

4.3 Area response 17

5 Data Acquisition Summary 18

6 Data quality 21

7 Processing results and data presentation 27

7.1 Reference receiver 27

7.2 Area response 30

7.3 Line response 34

7.4 Receiver responses 41

8 Summary 47

9 References 48

1 Introduction

A SeaBed Logging (SBL) survey was carried out in Sorell Basin, Australia. The data was acquired in August 2007. A total of 44 receivers were deployed along two lines.

The objective of this report is standard processing and visualization of recorded SBL data. The reader is, in addition, given a brief introduction to the SBL method.

2 SBL method

2.1 Subsurface resistivities

Seabed logging (SBL) surveys allow remote sensing of subsurface resistivity variations. Subsurface resistivities are controlled by the interplay between permeability, pore space geometry and pore fluid composition, and resistivities of permeable lithologies are strongly controlled by pore fluid resistivities. Pure mineral phases, air and hydrocarbons are resistors with resistivities > 10^9 Ωm while meteoric water and seawater are conductors with resistivities around 1 and 0.3 Ωm respectively (*Figure 2-1*).

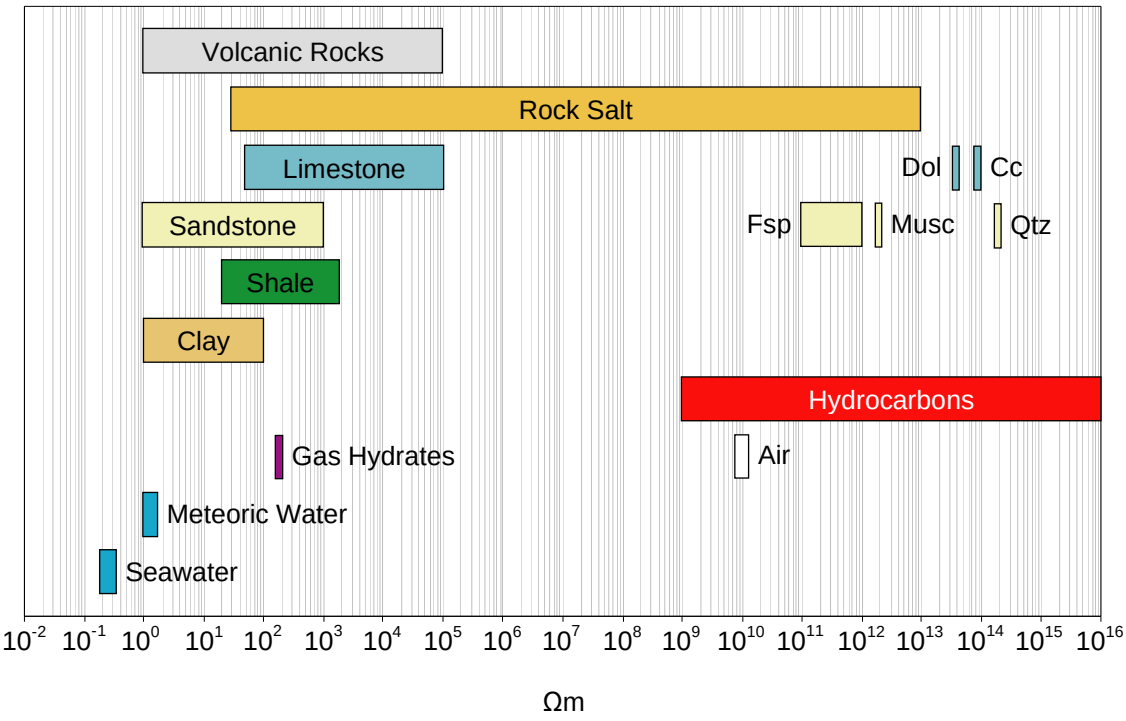

Figure 2-1 *Resistivity data for selected minerals, lithologies, hydrocarbons, air and water.*

Water wet sediments generally have resistivities in the range 1 – 2 Ωm while hydrocarbon bearing sediments have much higher resistivities generally around 50 - 1000 Ωm (Figure 2-2).

Hydrocarbon reservoirs can be detected by SBL, depending on resistivity properties, burial depth, reservoir thickness and 3D geometry factors. It is, however, important to note that lithologies such

as cemented sandstones, limestones, volcanic rocks and salt usually have high resistivities similar to hydrocarbon reservoirs or even approaching those of pure mineral phases (Figure 2-2).

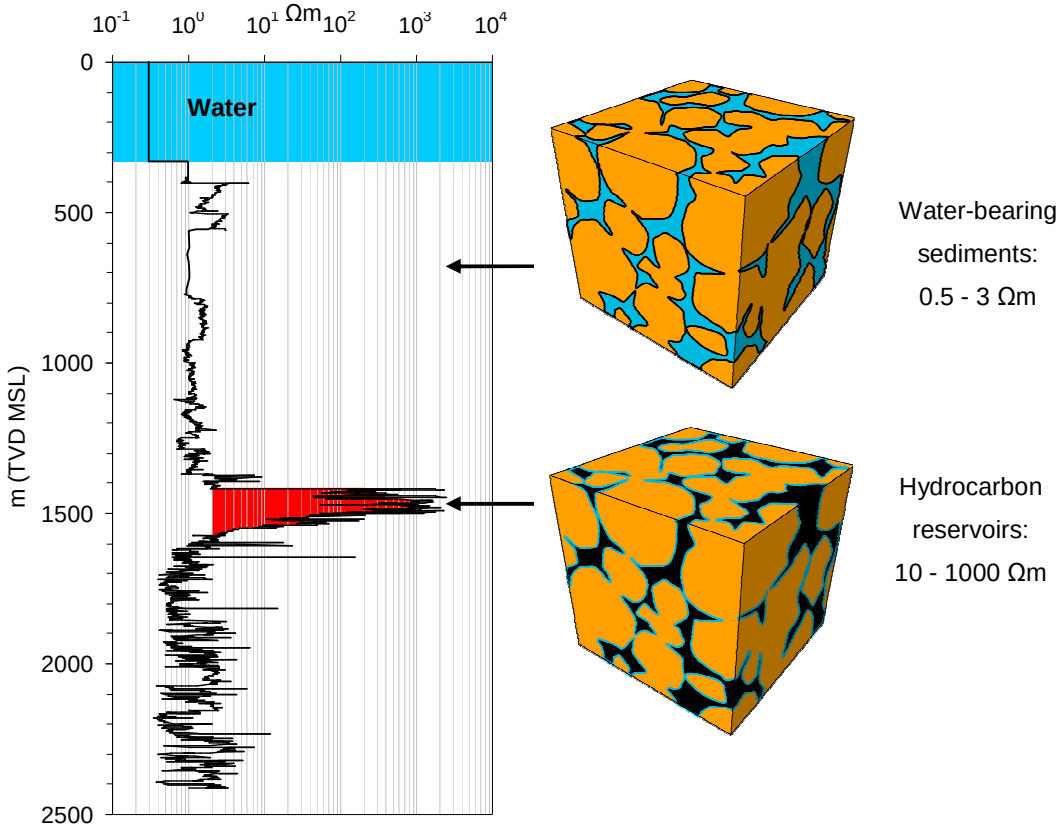

Figure 2-2 *Resistivity log from a borehole illustrating contrasting resistivities in water bearing sediments and a hydrocarbon reservoir. The resistivity of seawater, usually around 0.3 Ωm, is indicated in the upper part of the log curve.*

2.2 Transmission of electromagnetic energy

The basis of SBL is the use of a horizontal electric dipole source and an array of receivers positioned on the seabed (Figure 2-3). The dipole emits a low frequency electromagnetic signal both into the seawater column and downwards into the subsurface.

The signal, recorded by an array of seabed receivers consists of different contributions. Direct energy travels from the source to the receiver without subsurface interaction. However, due to the large attenuation in sea water, this contribution will only affect the results at very short offsets. Energy being refracted at the water/sediment interface and travels within the shallow sediment layer will also be recorded by the receivers. The combination of these two contributions is

referred to as “direct wave” (marked yellow). Another contribution, without subsurface interaction, is the energy refracted at the sea-air interface, referred to as “air wave” (marked green). A last contribution is represented by the energy travelling in deeper parts of the subsurface, due to high resistive layers (marked and red). Depending on source-receiver distance, subsurface structure and water depth, the three contributions mentioned above will dominate the recorded signal at different offsets. The “direct wave” will dominate recorded signals at relatively short source-receiver offsets. Energy refracted along the sea-air interface will generally dominate the recorded signal at relatively large source – receiver offsets. The offset dependence for the “air wave” is strongly influenced by the water depth, but also by subsurface resistivity and the signal frequency. When the water depth is large (more than about 1500 m) only a minor contribution to the recorded signal is seen for offsets less than 10 km. This contribution increases as the water depth decreases.

Energy which is travelling through deeper parts of the subsurface will affect the recorded signal from a certain offset range, depending on the burial depth of the refracting interface. A high resistivity subsurface layer such as a hydrocarbon reservoir will refract electromagnetic energy, causing an increased return signal from the subsurface recorded by the receivers (Figure 2-3).

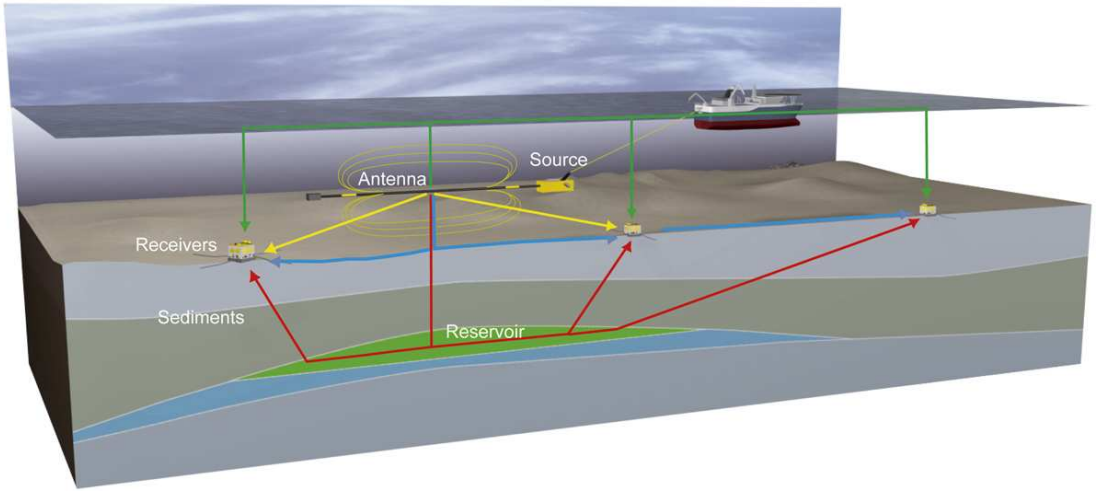

Figure 2-3 *Schematic representation of transmission paths for electromagnetic energy between source and receivers positioned over a high resistivity hydrocarbon reservoir.*

3 Data processing methodology and procedures

The acquired raw data are initially calibrated in time domain. This is done to relate the recorded signal (counts) to the physical field present at the receiver antennas and magnetic coils at the time of measurement. In principle, this is the reverse process to treatment of data from antenna registration to media storage. Calibrated time domain data are subsequently converted to netCDF format. netCDF is an open source format originally designed to give access to a variety of data types. One file is written for each receiver. Hence, each receiver is a stand-alone dataset, as every file contains receiver data, source data, navigation data and header information.

3.1 Standard processing

3.1.1 Demodulation

Receiver data are recorded in the time domain. The time domain electromagnetic data are transformed to frequency domain through a Fourier transform, extracting the frequencies of interest. The relevant frequencies depend on the source signature used for acquisition, as well as data quality. Transform windows are centred at user defined regular offset intervals, normally in time steps corresponding to 100 m of Tx movement. The length of the transform window (number of periods, np) is generally given by (rounded up to nearest integer)

$$np = (L \cdot f)/(2v)$$

where f is source base frequency, v denotes towing speed and L is the horizontal electric dipole (HED) source length. However, this window can be increased in order to increase signal-to-noise ratio (S/N), either as a constant length window or as a function of offset. Additionally, a taper can be applied in the Fourier transform window to increase S/N.

3.1.2 Scaling

The phase of the source current is used to obtain absolute phase data, meaning that the phase of the E-field is zero at zero Tx-Rx offset. The current amplitude is accounted for through normalization by the dipole current moment, which is defined by the product of current amplitude (in frequency domain) and the HED length. The frequency filtered receiver responses are divided (normalized) by the current moment for the corresponding frequencies, correcting for any changes in source current amplitude during acquisition. The dipole moment is a complex entity.

3.1.3 Channel drop/averaging

Receivers are equipped with two independent electric channels in the X direction and two in the Y direction. Due to this, redundant channels may either be summed or a channel with a deficient S/N may be omitted. This decision is based on QC of amplitude and phase data in the frequency domain. If two channels have different noise level, the noisy channel is dropped. If they have the same overall noise level, the two channels will be averaged in order to increase S/N.

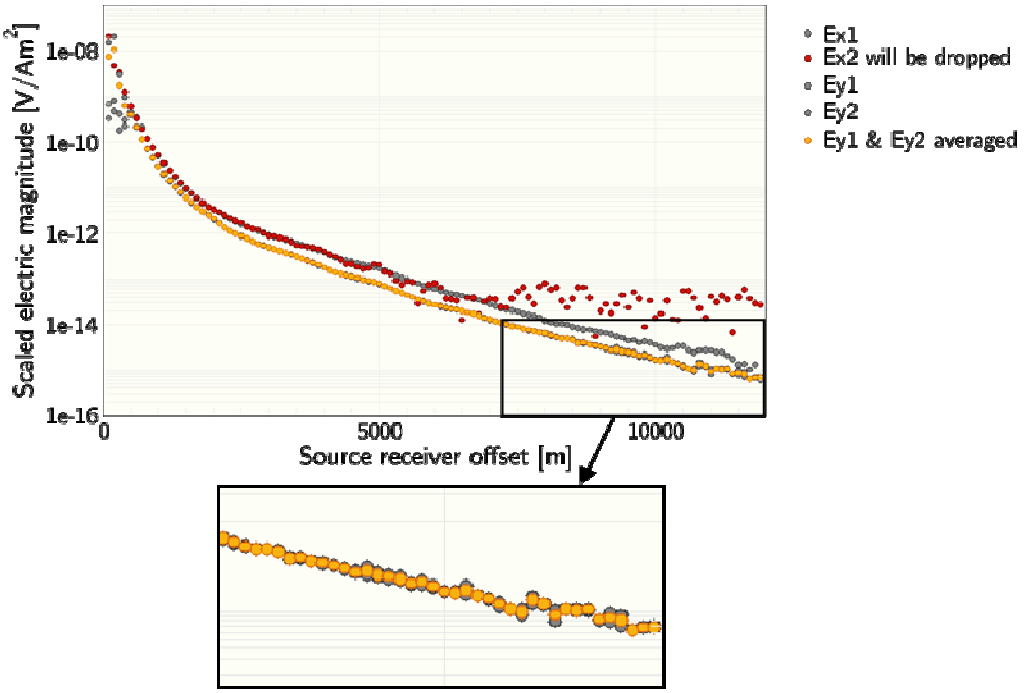

Figure 3-1 An example showing channel drop and averaging.

3.1.4 Inline rotation

After deployment, the receivers sink freely to the seafloor. Consequently, the X and Y antenna orientation is arbitrary. The size of the electromagnetic field at the antennas depends on their orientation relative to the transmitted field. For any given angle of the receiver antennas they measure the legs of the total electromagnetic vector field. Based on this, the antenna orientation compared to the transmitted field can be determined if the receiver is positioned in-line (along the x-axis) with the transmitted electromagnetic field (given the source is an x-directed dipole). In this case the total field will be dominated by the Ex and Hy components on behalf of the Ey and Hy components, and the rotation angles are computed through a maximization of Ex and Hy.

The angles are calculated for real data at given offsets. The methodology used usually gives consistent rotation angles for all offsets and also consistency between the independent calculations of electric and magnetic data.

An example of data before and after rotation is given in Figure 3-2, showing electric and magnetic MVO. After rotation the electric Ex channel and magnetic Hy channel are the strongest in magnitude.

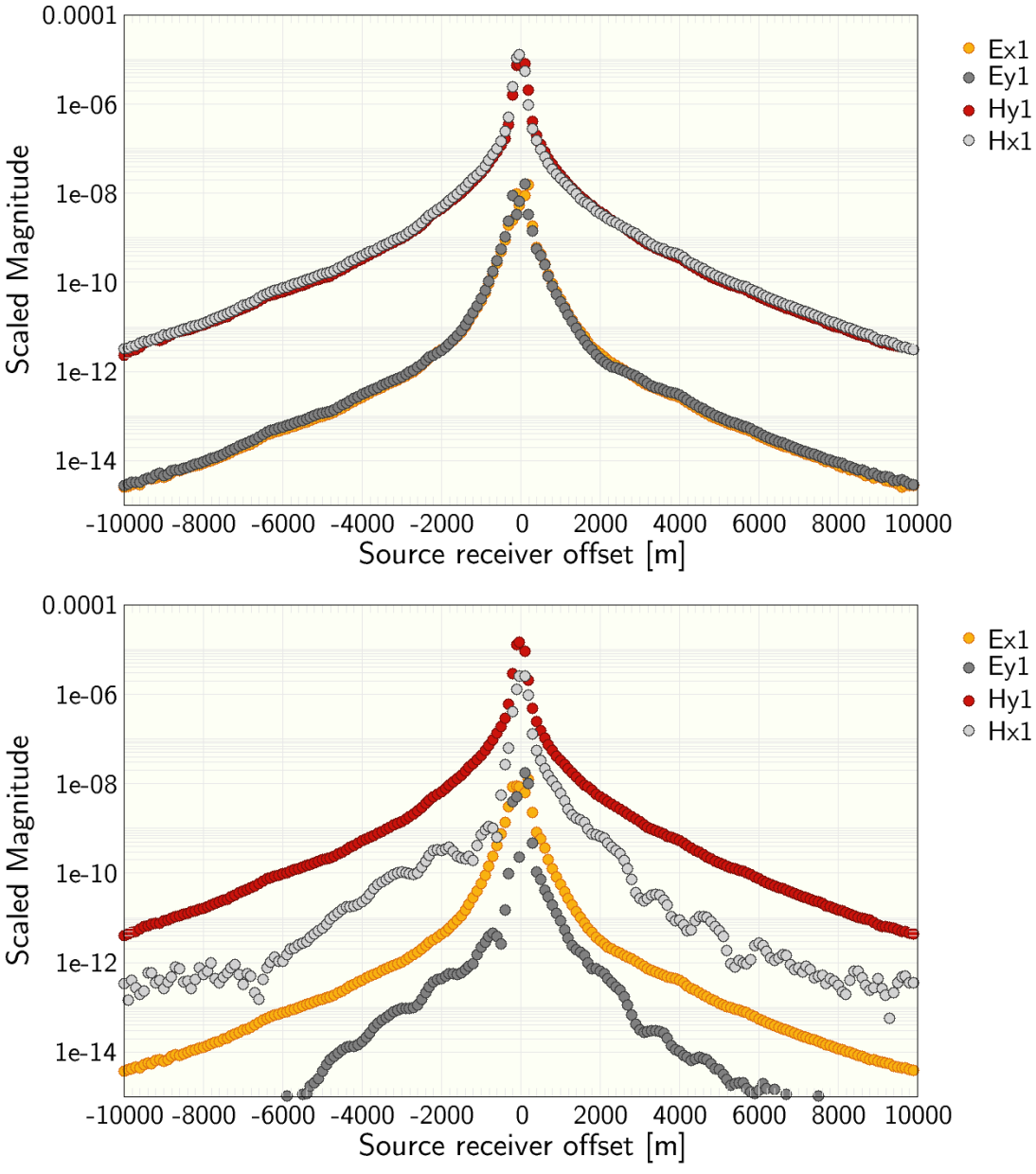

Figure 3-2 *Electric and magnetic MVO data at frequency 0.25 Hz before (upper) and after (below) rotation for one receiver.*

3.2 Up-Down separation

Up-Down separation decomposes the electromagnetic field into up-going and down-going components. SBL measurements are affected by fields coupled into the air above the sea surface and propagating along the sea-air interface with small to no attenuation. In shallow water the attenuation by propagation in the water column is small and the contribution from the air-water interface becomes a significant problem as it masks possible subsurface responses. At the receiver, the air wave is a part the down-going field, but it interferes with the up-going fields from the subsurface. The offset at which the energy from the air-water interface starts to dominate the recordings depends on water depth, frequency and subsurface resistivity responses. Up-Down separation is a method to attenuate the down-going components, including MT noise, in the receiver data. The algorithm assumes plane waves travelling in the z-direction (i.e. horizontal slowness parameters $p_x = p_y = 0$). This assumption may be valid at large offsets only, but generally the validity is dependent on water depth and subsurface geology. In order to decompose the electromagnetic filed both the horizontal electric and magnetic field components are needed. Hence, Up-Down separation can only be applied to receivers equipped with both electric and magnetic sensors.

An example of successful application of Up-Down separation is shown in Figure 3-3. A strong decline in the magnitude can be seen at far offsets for the electric magnitude where the field propagating in the water completely dominated the data before up-down separation.

The air-wave related event is characterized by a near zero phase slope for the higher offsets in the un-separated PVO data (bottom picture). A strong shift towards the far offsets and a linear behavior is seen after up-down separation. Additionally, the phase slope is increased at the intermediate offsets after up-down separation, indicating the attenuation of the high velocity component as well.

Up-Down separation was applied to the Wolseley dataset due to the presence of shallow water in the survey area.

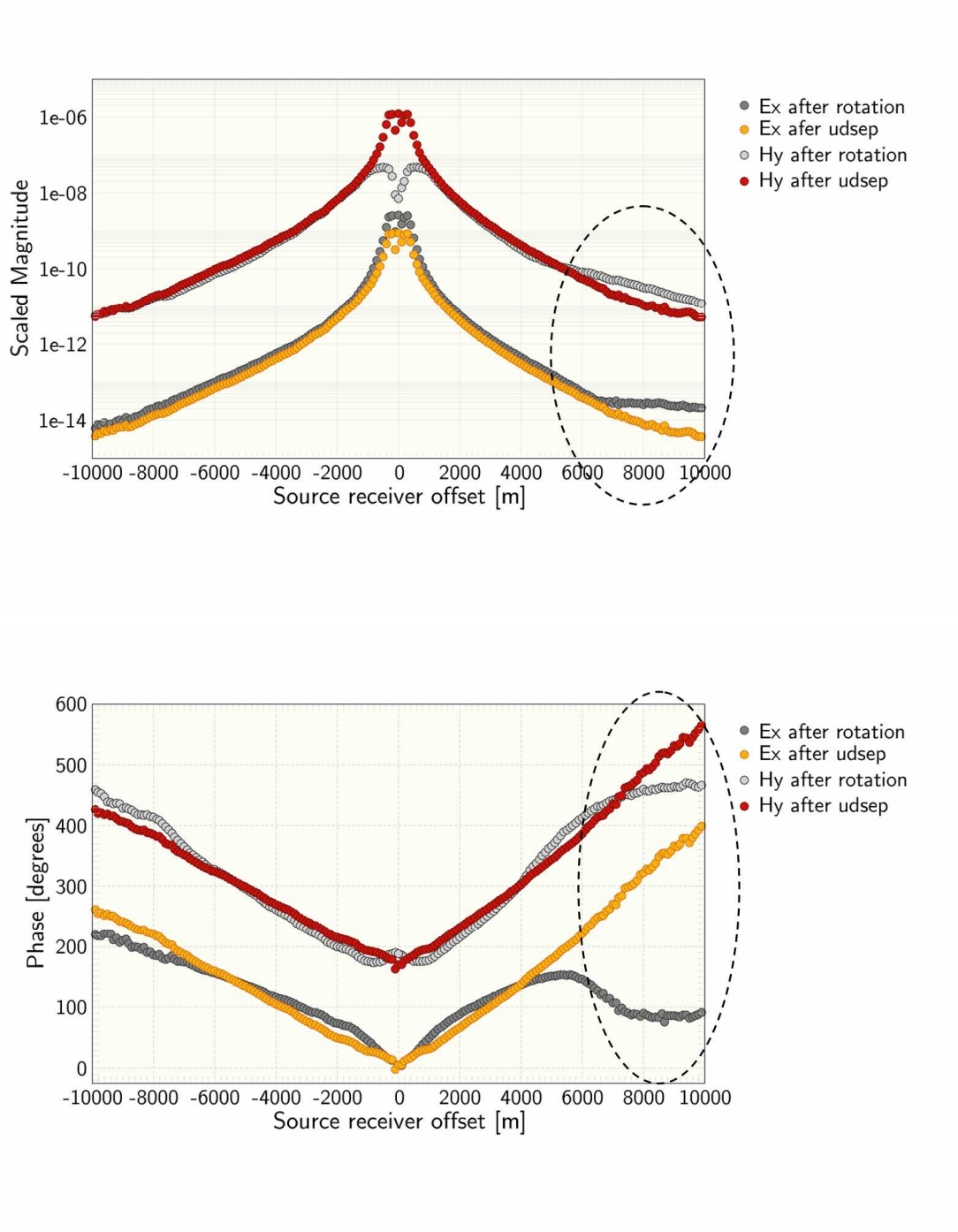

Figure 3-3 *Electric MVO (upper) and PVO (lower) data at base frequency 0.25 Hz. Data before and after Up-down Separation are red and black respectively.*

3.3 Data Processing Sequence

The following flow chart visualizes the applied processing flow and the processing parameters applied to this survey.

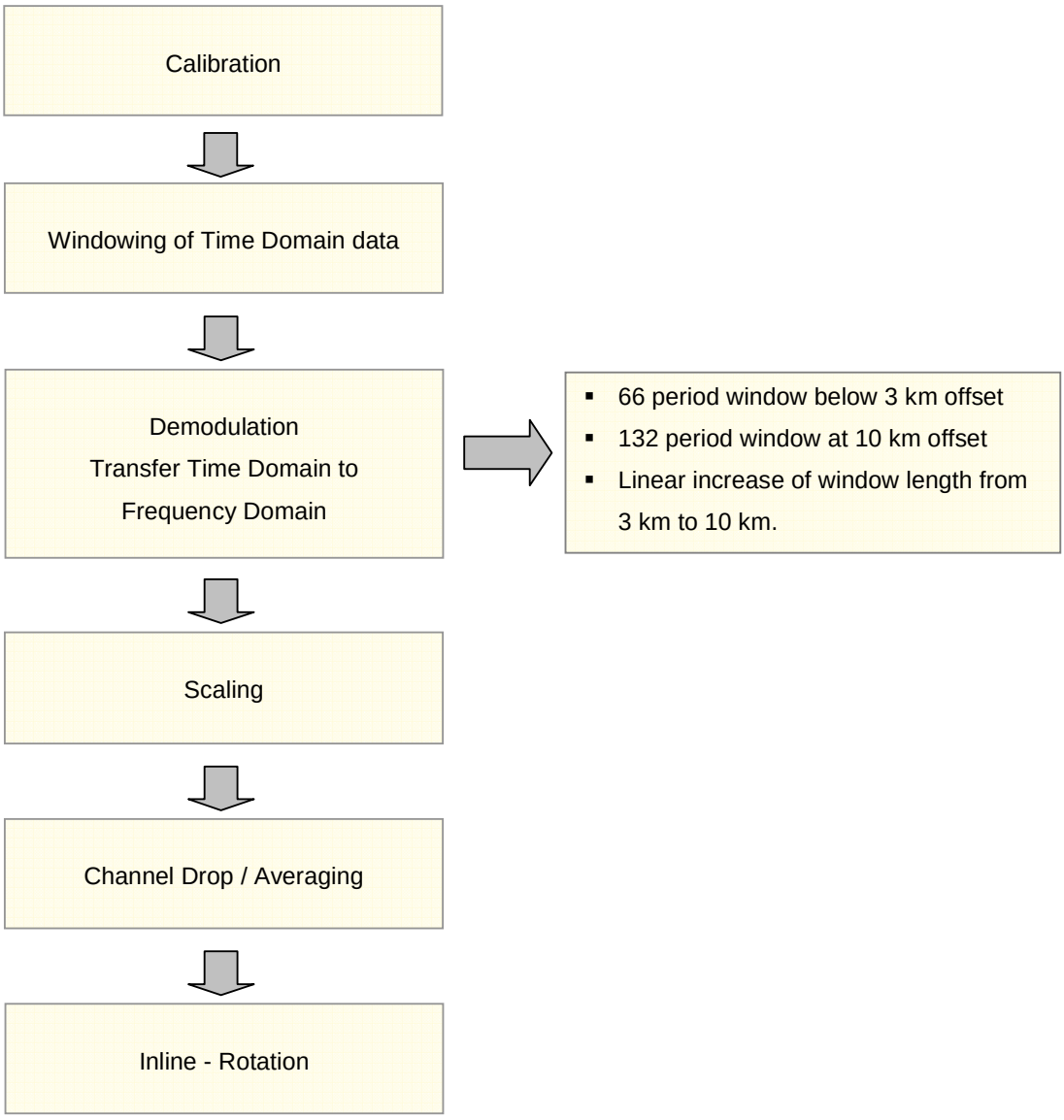

Figure 3-4 Flow chart showing the processing flow and relevant parameters.

4 Data presentation

4.1 Receiver response

The recorded time series is, through a Fourier transform, converted into magnitude and phase data which are presented as Magnitude Versus Offset (MVO) and Phase Versus Offset (PVO) plots.

To evaluate the MVO and PVO data recorded over a possible subsurface resistivity anomaly, it is usual to compare this with MVO and PVO data recorded in an area with no expected subsurface resistivity anomalies. This is done by placing a reference receiver well outside the selected target. The resulting MVO and PVO curves can then be compared.

Figure 4-1 and Figure 4-2 show MVO and PVO data from a receiver located on the edge of a subsurface hydrocarbon accumulation. This receiver shows a clear asymmetry when measuring over the accumulation (right side), as opposed to the measurements outside the accumulation (left side). Compared to a reference receiver, MVO data show an increase between 4 and 9 km offset (on the right side) due to refraction of electromagnetic energy from the high resistivity reservoir. Similarly, PVO data show a decreased slope, compared to the reference receiver, between 3 and 7 km offset, again reflecting the interaction with a high resistivity subsurface layer.

The evaluation of MVO and PVO responses like those illustrated in Figure 4-1 and Figure 4-2 is essential in the interpretation of SBL data. In order to enhance visual interpretation of receiver data, each receiver is normalized against a reference receiver. This procedure generates two new plots, named normalized magnitudes versus offset (NMVO) and phase difference versus offset (PDVO). An illustration is given in Figure 4-3. The normalised magnitude response is calculated by dividing the magnitude recorded at a particular offset with the magnitude recorded at the same offset by the reference receiver. As reference for this procedure is a polynomial best fit curve for the measured data of the reference receiver used, removing possible noise influence in the reference data. In order to compensate for varying conditions during measurements, normalized magnitude data are adjusted so that values are equal at near offsets (e.g. 1 km). This is referred to as “shifted NMVO”. The phase difference is calculated by subtracting the phase at a given offset from the phase data measured at the same offset by the reference receiver. Accordingly, increased subsurface resistivities will be manifested as NMVO values > 1 and PDVO values < 0.

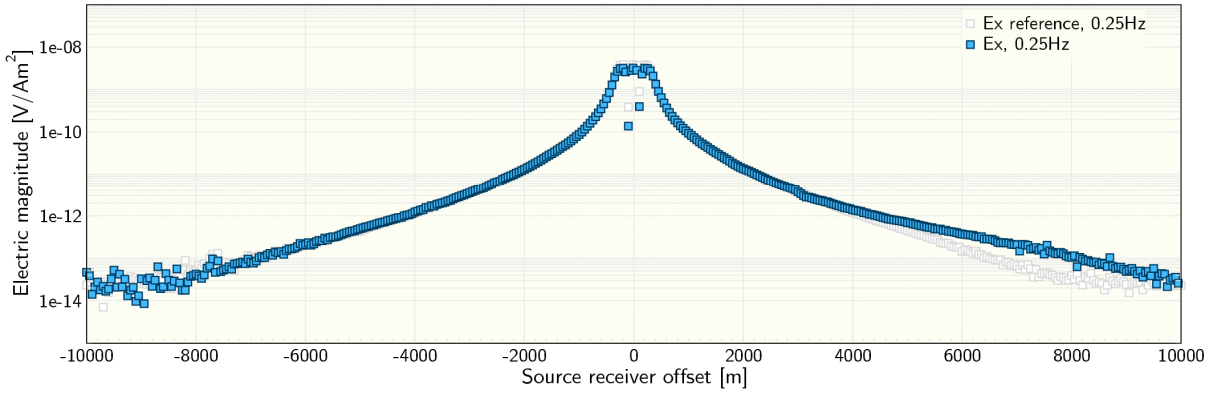

Figure 4-1 *Example of measured magnitude versus offset (MVO) for a receiver recording a subsurface hydrocarbon reservoir. Magnitudes for the reference receiver are shown as grey open symbols.*

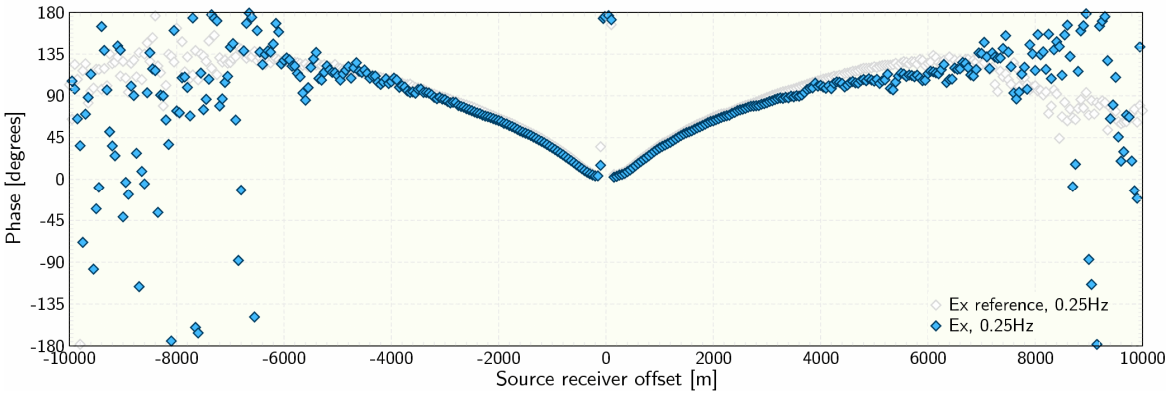

Figure 4-2 *Example of measured phase versus offset (PVO) for a receiver recording a subsurface hydrocarbon reservoir. Magnitudes for the reference receiver are shown as grey open symbols.*

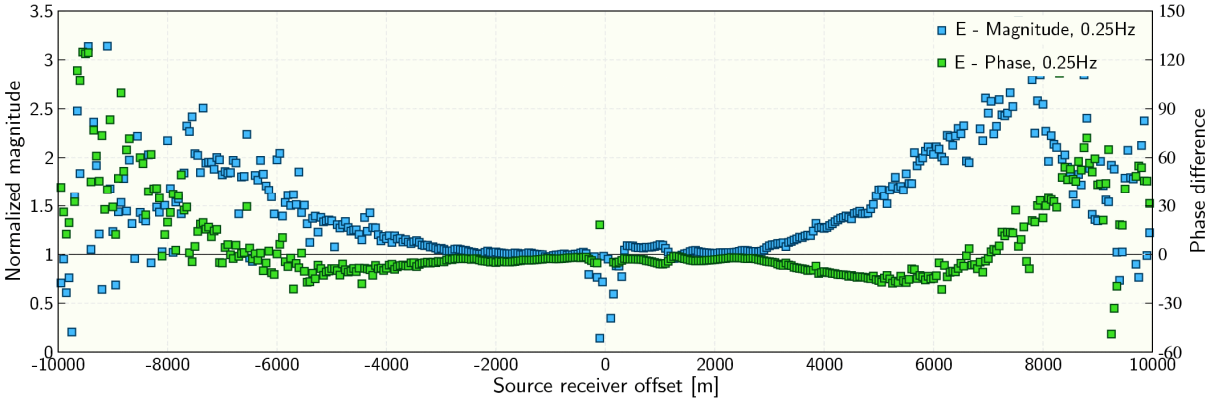

Figure 4-3 *Example of normalized magnitude versus offset (NMVO) and phase difference versus offset (PDVO) for a receiver recording a subsurface hydrocarbon reservoir.*

The exact offset range recording the maximum deviation from MVO and PVO data for the reference receiver will mainly depend on burial depth and thickness of the subsurface resistivity anomaly, the resistivity contrast between the resistivity anomaly and the overburden, the water depth and the horizontal displacement. Shallow resistivity anomalies will tend to generate MVO and PVO anomalies at nearer offsets. Shallow water depths may cause the data to be controlled by a strong air wave signal at intermediate to far offsets, thus subduing subsurface anomalies beyond this offset range.

4.2 Line response

4.2.1 Line summary plots

Inline variations in MVO and PVO are visualised by displaying the average NMVO and PDVO values within a chosen offset range for all receivers along a line. These offset ranges are typically chosen as 0.5 km to 1 km windows depending on data quality. NMVO and PDVO attributes are sampled as median values within these windows. Line summaries are generated by posting the median NMVO and PDVO values at "common midpoint" position (½ source – receiver offset) as illustrated in Figure 4-4. The well defined inline position of the NMVO and PDVO anomaly illustrated in the figure reflects the location of a subsurface high resistivity hydrocarbon reservoir. Line summary figures can also include data on receiver position and water depth to correlate to possible effects of bathymetry variations.

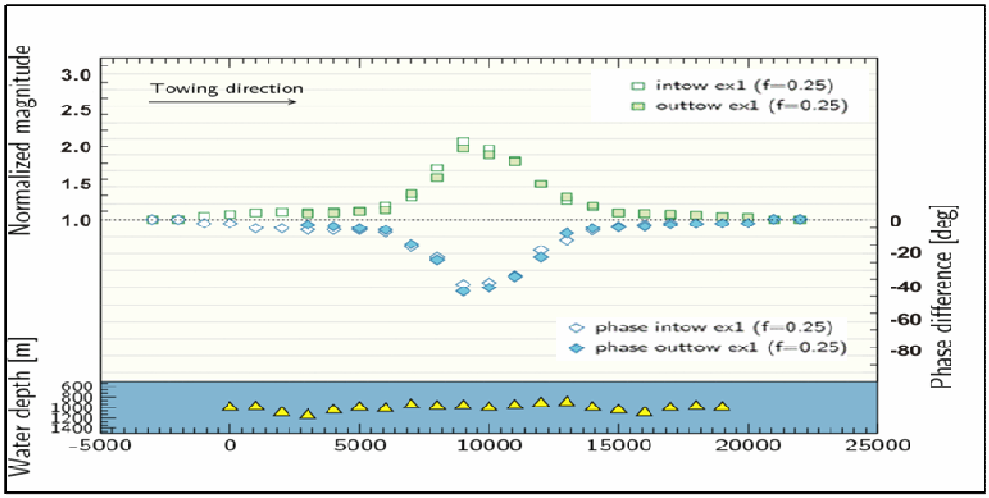

Figure 4-4 *Example of line summary figure above a subsurface high resistivity hydrocarbon reservoir displaying inline NMVO (green symbols) and PDVO data (blue symbols) together with receiver positions and bathymetry.*

4.2.2 Surface consistency

To evaluate MVO and PVO responses potentially recording a deeply buried HC reservoir, it is important to identify anomalies linked to variations in near seabed parameters such as installations (e.g. well casings, example in Figure 4-5), abrupt changes in bathymetry (e.g. due to escarpments or channels) or shallow gas. MVO and PVO responses controlled by near seabed parameters will tend to show up as abrupt, short wavelength changes in magnitude or phase at a particular inline location. Such anomalies can be identified by plotting MVO and PVO data for several receivers using the actual distance between the receivers. On this plot, anomalies as described above will show up along a vertical line, hence the name 'surface consistent plot' (scp) This plot can also be combined with bathymetry or seismic data. However, the edge of deeper resistive bodies may also show up as surface consistent, provided that the size of the body is large enough to be detected at the particular depth. An example of this is shown in Figure 4-5. For the receivers outside the reservoir, the point where the anomaly starts is surface consistent, while for the others it occurs at the same source-receiver offset. The same will apply for the case where the receivers are above a reservoir, while the source is towed across the edge. A drop in response is seen when crossing the edge, which will be surface consistent.

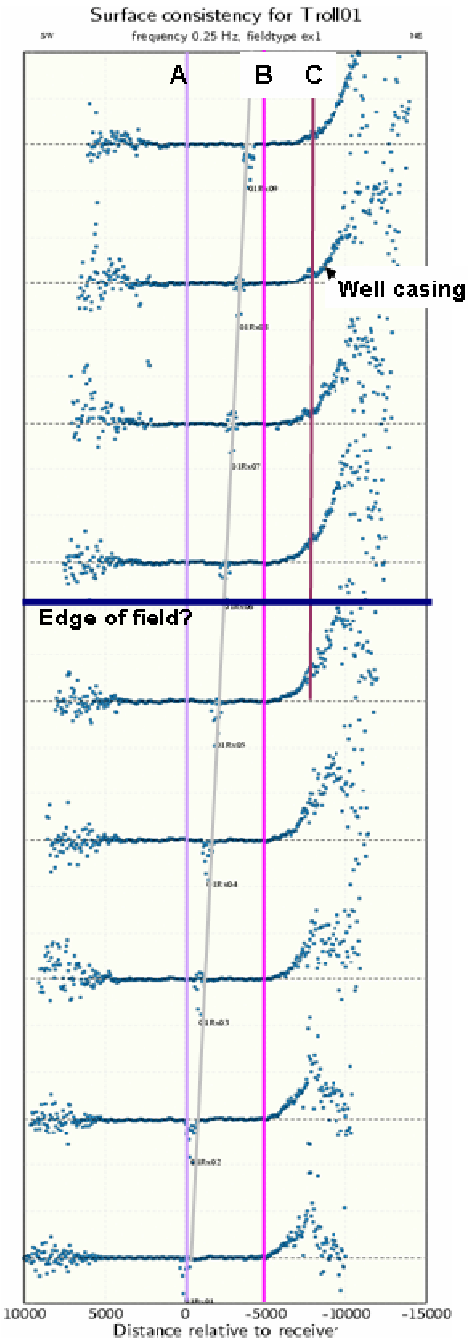

Figure 4-5 *NMVO data for multiple receivers plotted to identify surface consistent features. The receivers are plotted at the actual position relative to the lower receiver (Line 'A'). For the 5 lower receivers, the reservoir anomaly starts at a fixed inline position (Line 'B'), while for the upper 4, it starts at a fixed source-receiver offset. A small notch on some receivers (Line 'C') is believed to be caused by a well casing.*

4.3 Area response

Variations in MVO and PVO can be visualised by annotating NMVO or PDVO values on survey area maps for comparison with prospect- or field outlines, or to summarize data from several SBL lines (Figure 4-6).

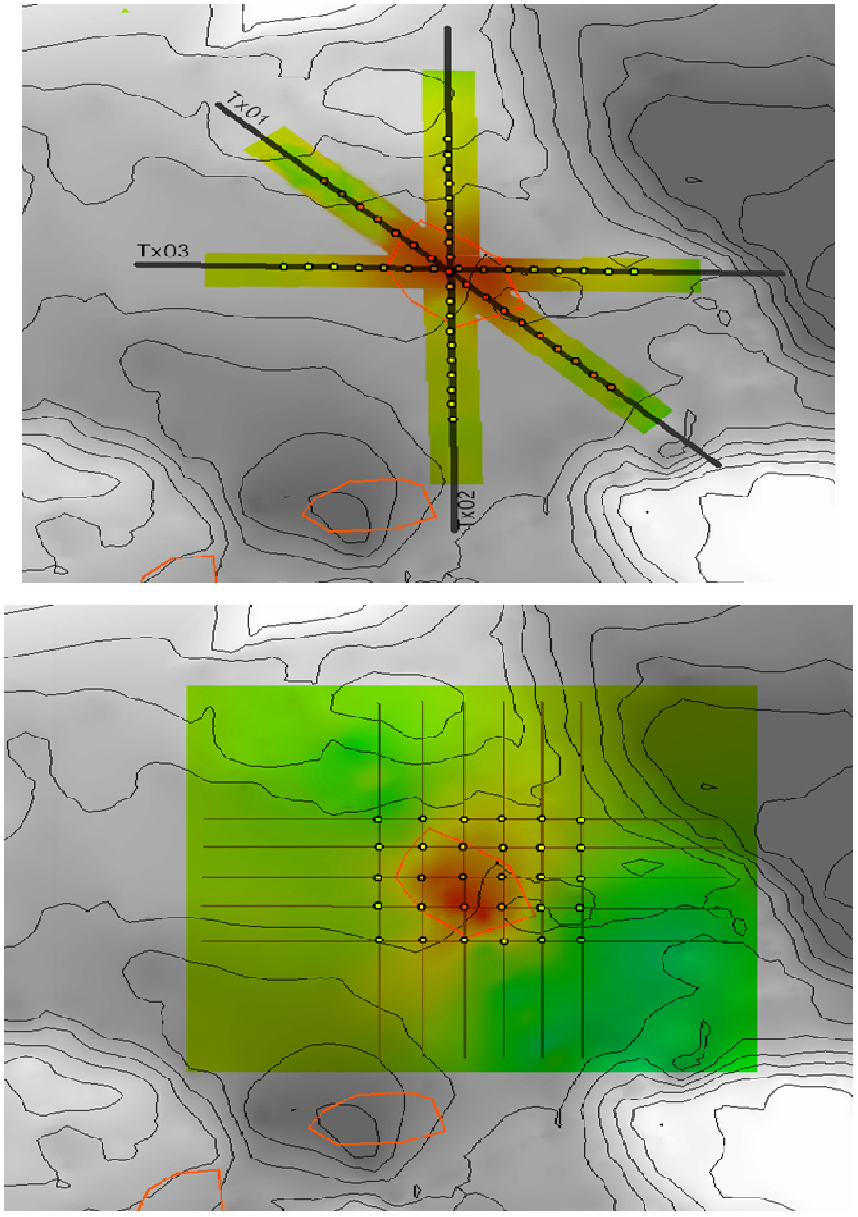

Figure 4-6 *Area summary showing NMVO data from Figure 4-4 posted together with field outline and a top reservoir map. The upper figure shows SBL 2D lines while the lower figure shows a SBL 3D scan.*

5 Data Acquisition Summary

A SeaBed Logging (SBL) survey was carried out in Sorell Basin, Australia. The data was acquired in August 2007. A total of 44 receivers were deployed along two lines. All receivers measured both the electric and magnetic field in two orthogonal directions (Ex, Ey, Hx and Hy) with redundant measurements for the electric field. Water depth in the survey area is large, varying from 1700 to 2500 meters.

A composite square pulse was used as the transmitter waveform (Figure 5-1), with a base frequency of 0.25 Hz. Current amplitudes at the seven most significant harmonics are given in Table 5.1.

All key acquisition parameters are summarized in Table 5.2 to Table 5.4. Receiver positions and transmitter lines are shown in Figure 5-2. A more detailed description of the survey is given in "Data Acquisition Report, Wolseley".

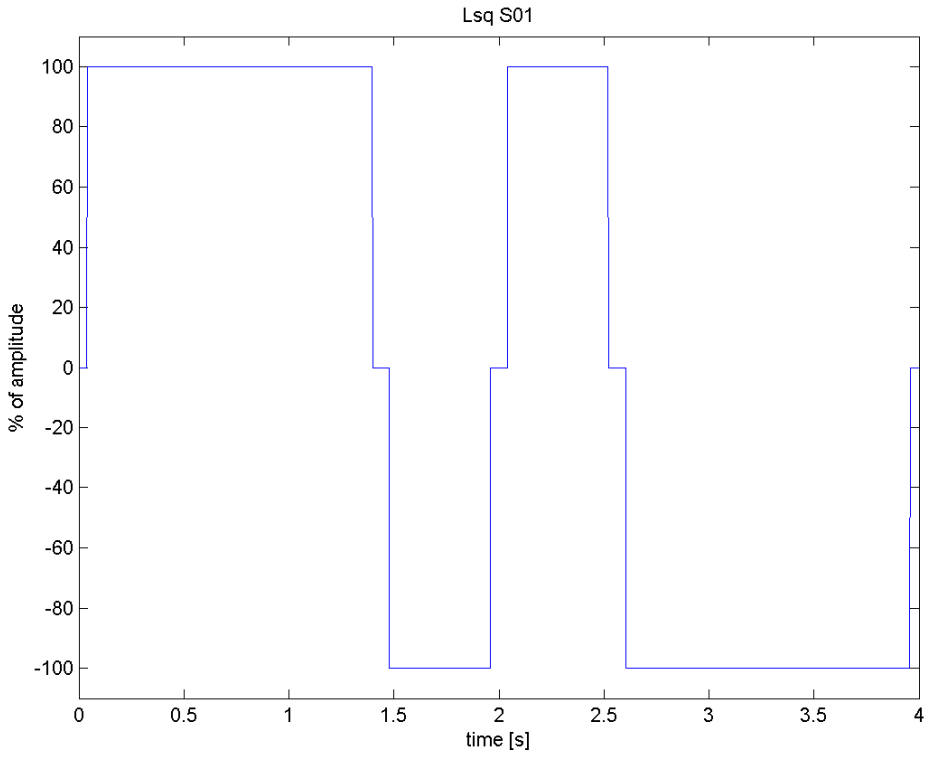

Figure 5-1 *Source waveform (time domain) designed for the Wolseley survey. One period (T) of the signal is shown.*

Table 5.1 Wolseley survey: Source waveform

Frequency	Current Amplitude (A)	Harmonic
0.25	800	1
0.50	750	2
0.75	364	3
1.00	581	4
1.25	65	5
1.50	85	6
1.75	157	7

Table 5.2 Wolseley survey: Operating statistics

Number of Tx-Lines	2
Total transmission kilometres*	91
Receivers deployed / recovered	43/44
Data recovery E-field	39/40 (97.5 %)
Data recovery H-field	39/40 (97.5 %)

* Exclusive aborted and retransmitted lines.

Table 5.3 Wolseley survey: Towline summary

	SOL		EOL		Heading	Tow line
Line	Easting	Northing	Easting	Northing	[deg]	[km]
Wolse01Tx01	707711.2	9969024.5	661101.2	5487578.1	276.78	62.1
Wolse02Tx01	700547.4	5498829.2	668607.2	5472218.3	228.89	41.6

Table 5.4 Wolseley survey: Source characteristics

Antenna Type	Horizontal electric dipole (HED)
Antenna Length	271.8m
Source shape	Composite square
Base frequency	0.25 Hz
Source current	1000 A

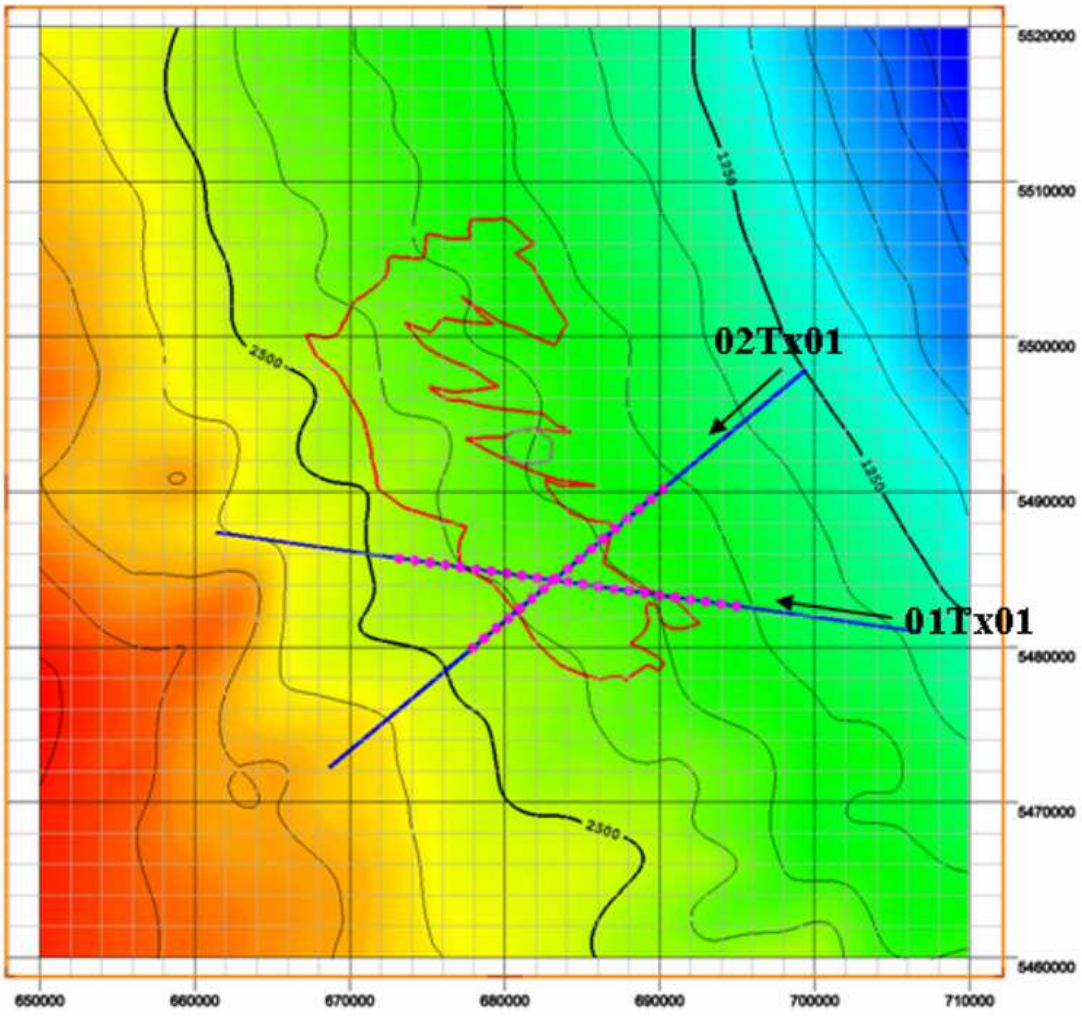

Figure 5-2 *Wolseley survey layout: Receiver positions and transmitter lines on a water depth map. The names of the towlines are placed at the start of line (SOL) locations.*

6 Data quality

High quality data were, in general, recorded for the Wolseley survey. The location of receiver 01Rx004 along towline Wolse01Tx01 is shown in Figure 6-1. A receiver measurement representative of the data quality in this survey is shown in Figure 6-2 to Figure 6-4, where the magnitude and phase responses display both the inline electric and magnetic field at 0.25 Hz (base frequency), 0.50 Hz (second harmonic) and 0.75 Hz (third harmonic). Receiver 01Rx004 from the synthetic model was chosen as the reference receiver for the dataset. The out-towing area of 01Rx004 represents the reference area. For the Wolseley survey, up-down separation was not performed due to the deep water. As expected, the offset ranges of high quality data are strongly dependent on frequency. The quality of the electric field measurements, in addition, is slightly higher than the magnetic field measurements.

The offset ranges where high quality data were recorded are summarized in Table 6.1. The offset ranges are based on visual inspection of data scatter on inline rotated data, magnitude and phase.

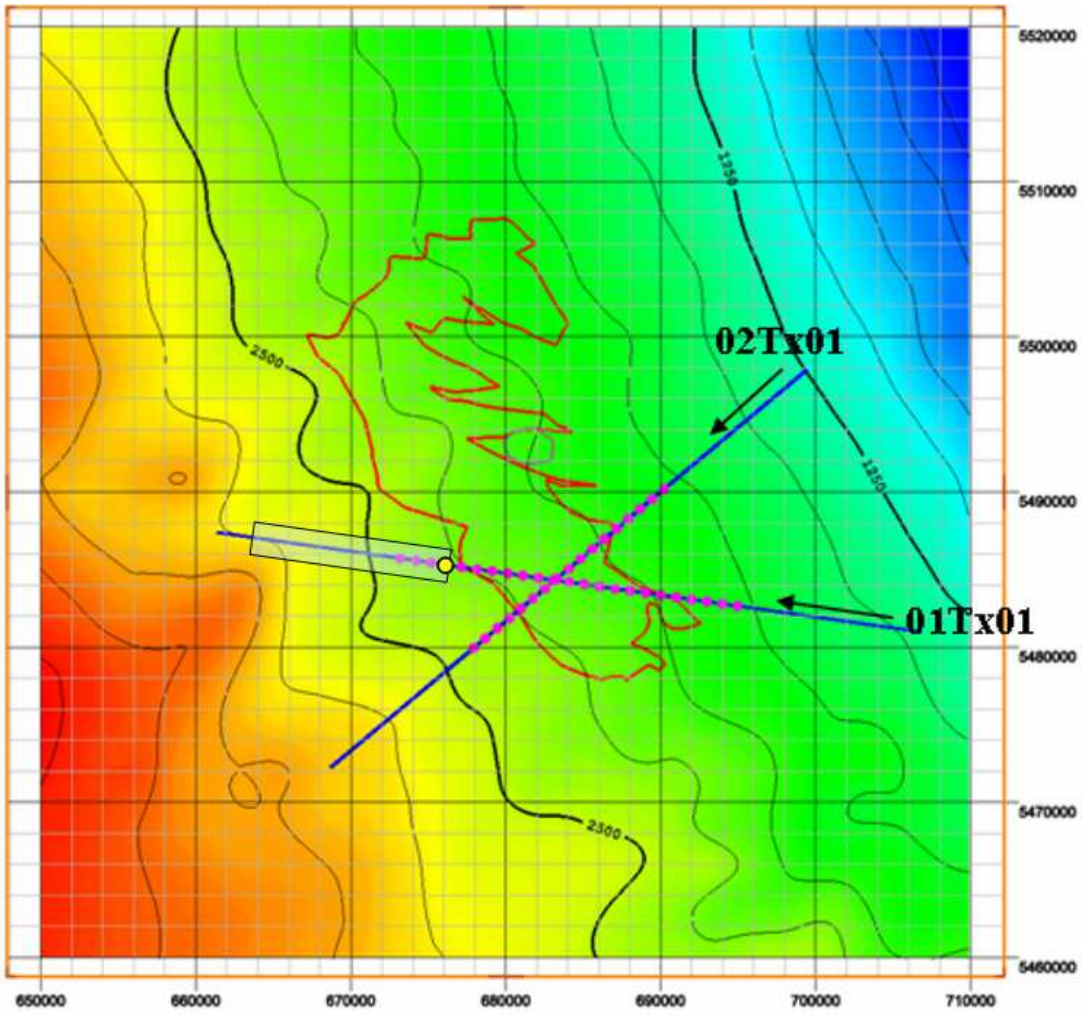

Figure 6-1 *Survey layout with receiver positions and towlines. The location of receiver 01Rx004 (yellow circle) is shown on the map together with the corresponding out-towing area.*

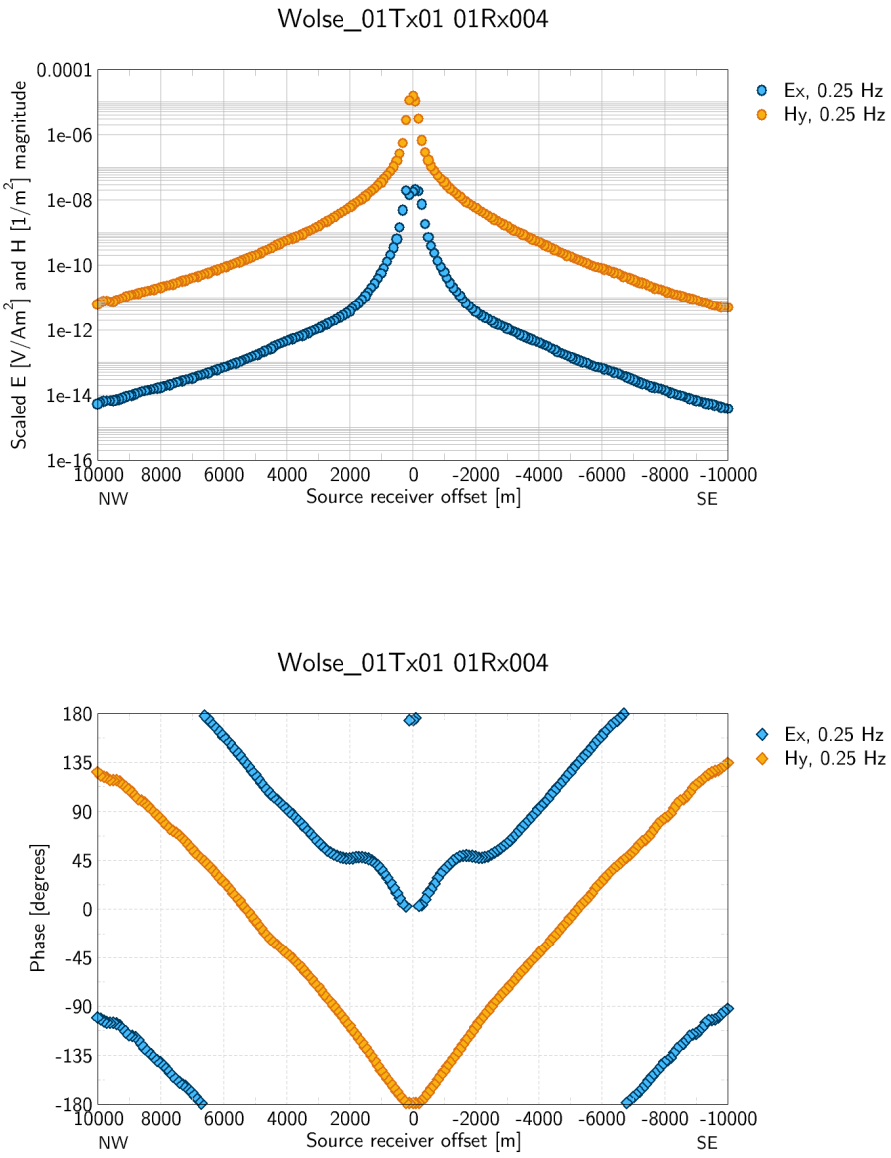

Figure 6-2 *Inline rotated electric / magnetic MVO (upper) and PVO (lower) for receiver 01Rx004 along Wolse01Tx01 at base frequency (0.25 Hz).*

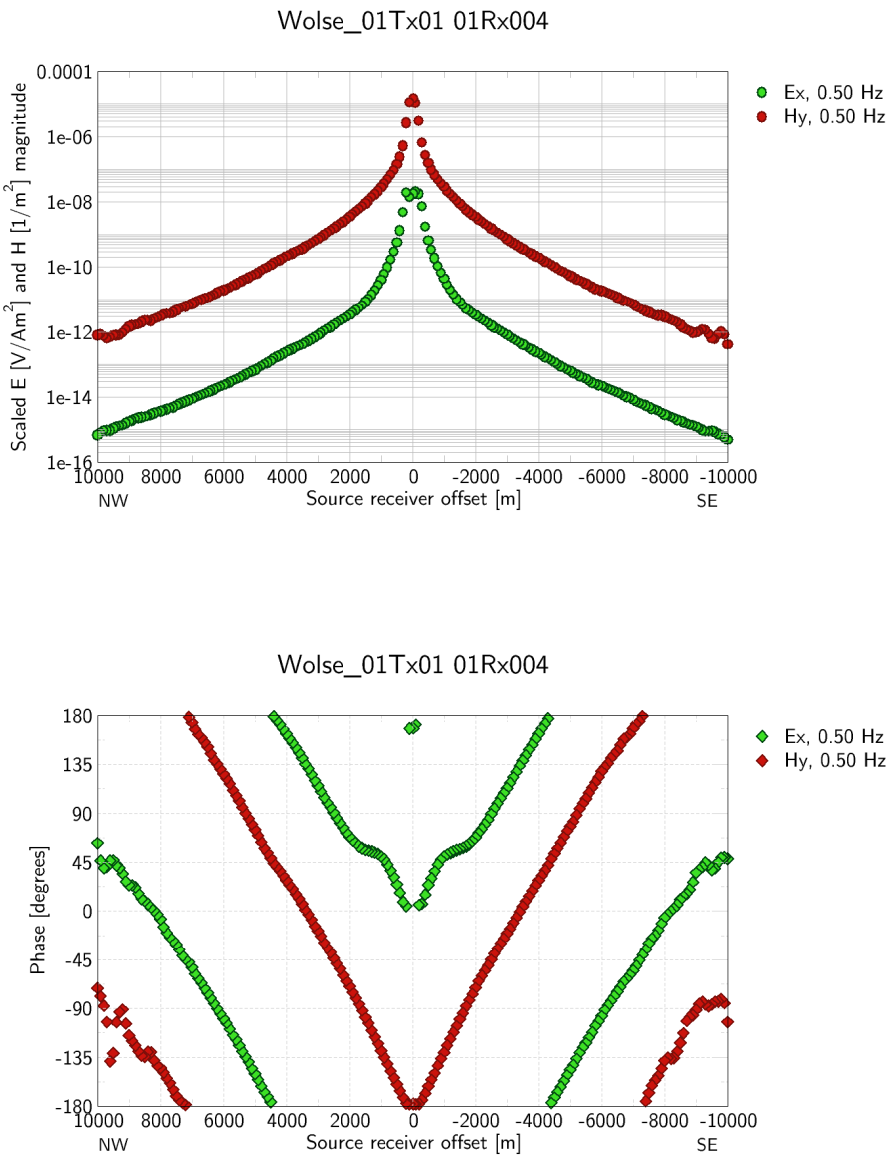

Figure 6-3 *Inline rotated electric / magnetic MVO (upper) and PVO (lower) for receiver 01Rx004 along Wolse01Tx01 at 2nd harmonic (0.50 Hz).*

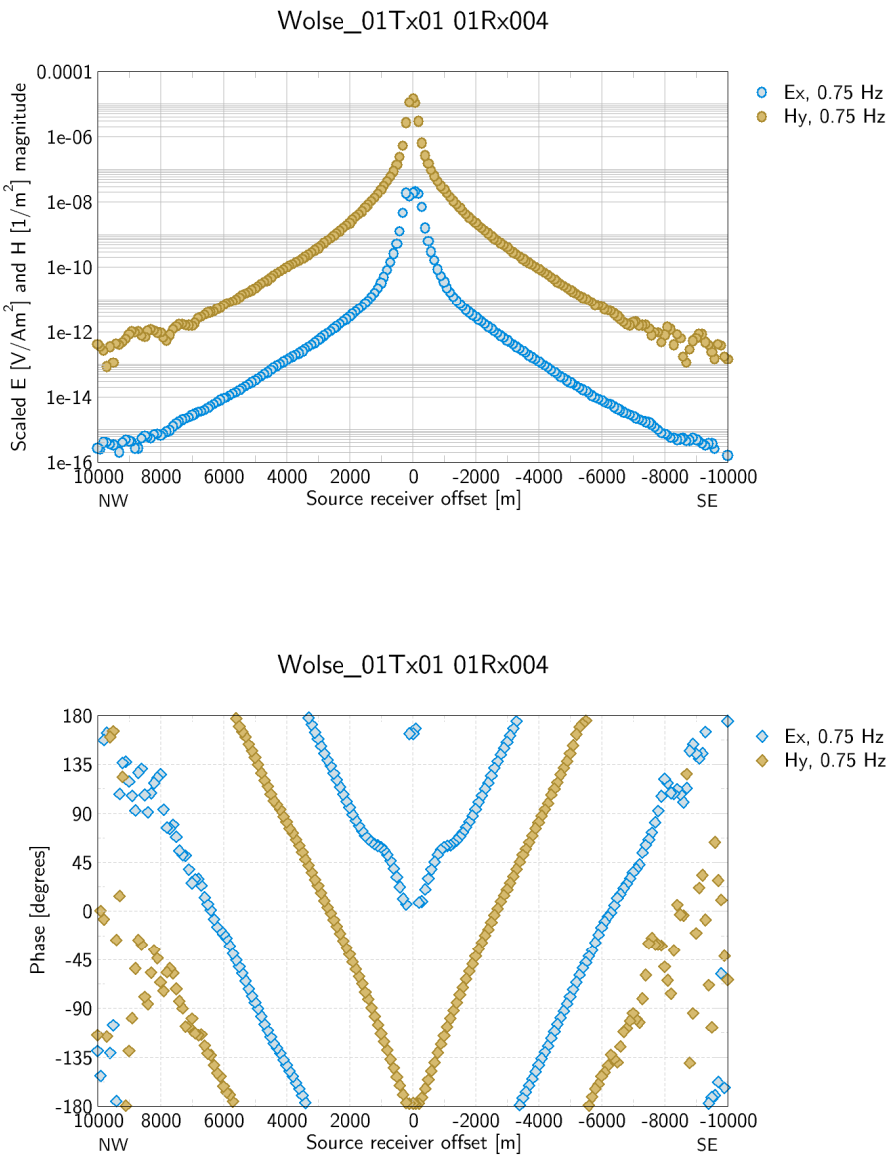

Figure 6-4 *Inline rotated electric / magnetic MVO (upper) and PVO (lower) for receiver 01Rx004 along Wolse01Tx01 at 3rd harmonic (0.75 Hz).*

Table 6.1 *Offset ranges where high quality data are recorded. The offset ranges are obtained by visual inspection of individual MVO and PVO responses.*

		Offset range [km]	
Lines	Frequency [Hz]	Electric field	Magnetic field
Wolse01Tx01 Wolse02Tx01	0.25	10	10
	0.50	9.5	8
	0.75	7	6
	1.00	6.5	5.5
	1.25	5	4
	1.50	5	4
	1.75	4.5	4

7 Processing results and data presentation

Processed data, as described in Chapter 4, are presented as both individual receivers and receivers combined along towlines. Normalized magnitude and phase difference are attributes which are used to highlight resistive anomalies. They are obtained by referring each recorded receiver response to a reference receiver. In this chapter, offset and frequency dependency of these magnitude and phase anomalies will be analyzed, as well as the strength and geographic location. The data presentation methodology used here is described in Chapter 4.

The water depth is deep, varying from 1700 to 2500m in the survey area. Up-down separation has therefore not been performed.

Inline data is presented below.

7.1 Reference receiver

The out-towing area of receiver 01Rx004 along towline Wolse01Tx01 was selected as a reference area for a synthetic reference receiver in the Wolseley survey (Figure 7-1).

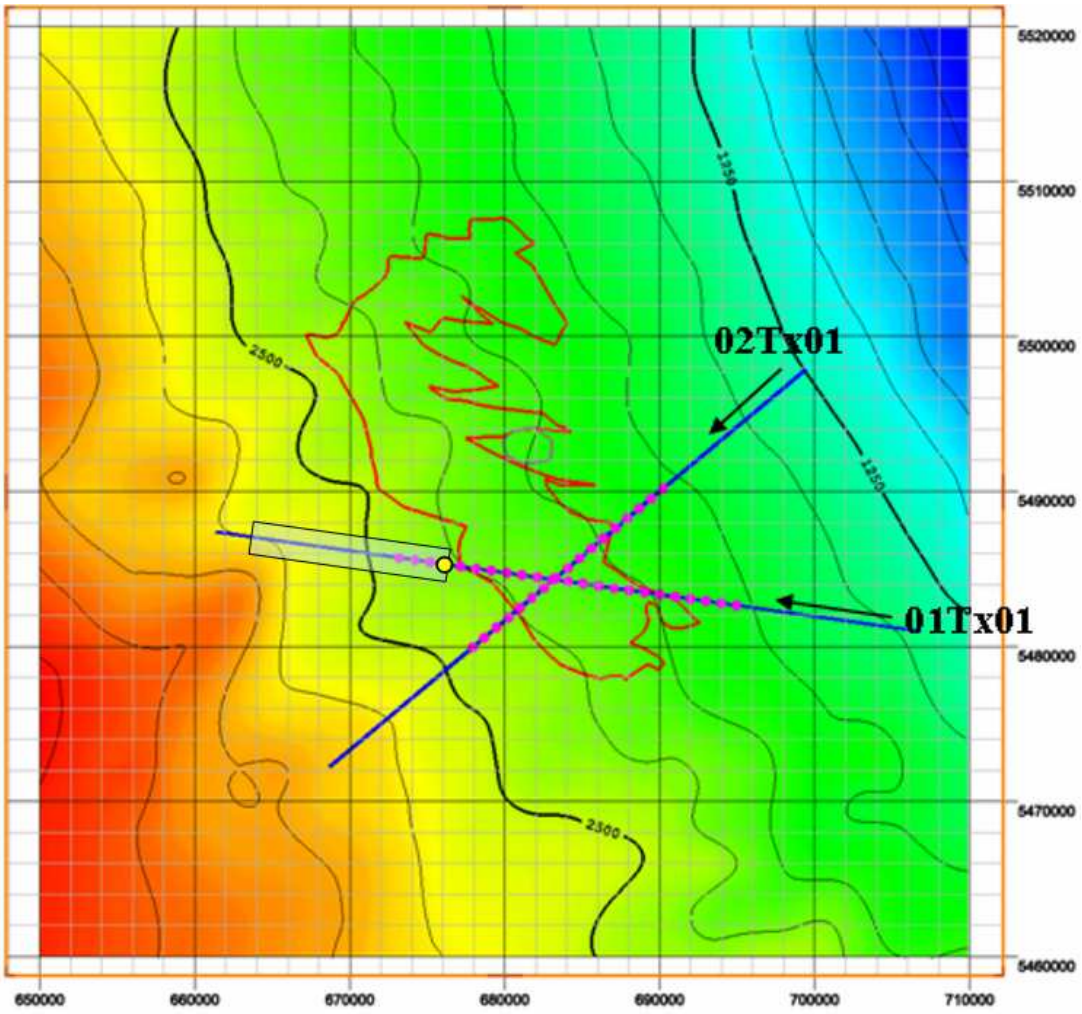

Figure 7-1 *Survey layout map with reference area (black rectangle), the out-towing side of receiver 01Rx004 along Wolse01Tx01.*

7.1.1 Standard processing

Standard processed responses for the reference area are shown in Figure 7-2. Dashed lines represent the response for each of the three frequencies 0.25 Hz (base frequency), 0.50 Hz (second harmonic) and 0.75 Hz (third harmonic). The reference receiver is a synthetic model which represents the out-towing area of receiver 01Rx004 along towline Wolse01Tx01.

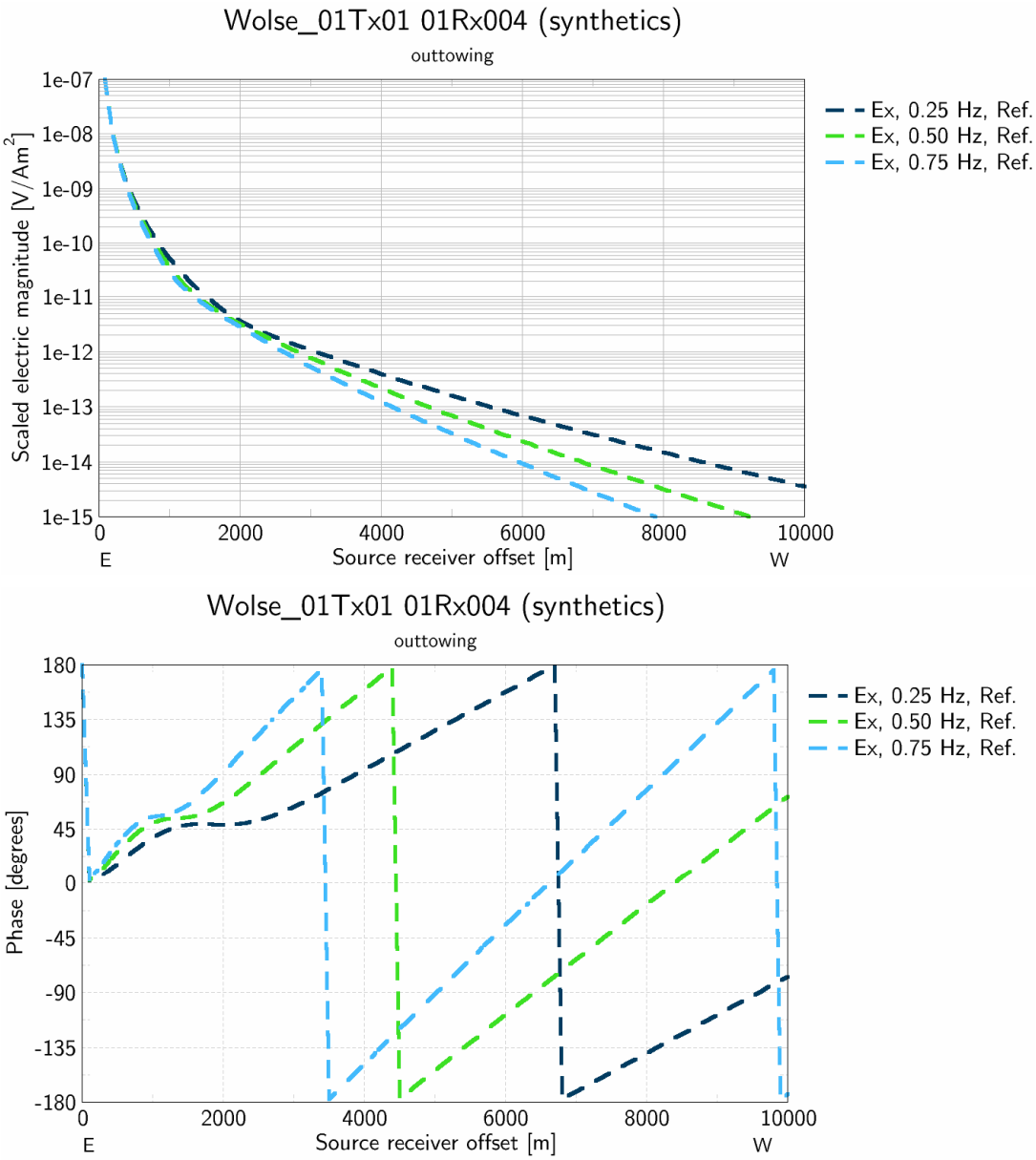

Figure 7-2 *Standard processing - Magnitude (upper) and phase responses (lower) for 1st, 2nd and 3rd harmonic recorded by the reference receiver 01Rx004 (synthetics) out-towing.*

7.2 Area response

7.2.1 Standard processing

The area responses for the Wolseley survey are summarized in Figure 7-3 to Figure 7-5, where the standard processed normalized electric magnitudes at selected frequencies and offsets are shown on a top of seabed map. At 3.5km offset, weak anomalies appear at the centre while weak to moderate anomalies are observed at SW of Wolse02Tx01 at 0.25Hz. This response also increases in strength with increasing frequencies. At 8km offset for 0.25Hz, weak anomalies appear at centre while weak to moderate anomalies appear at both ends for the two lines. This response also increases in strength with increasing frequencies. Only the electric data is presented due to the quality of the data.

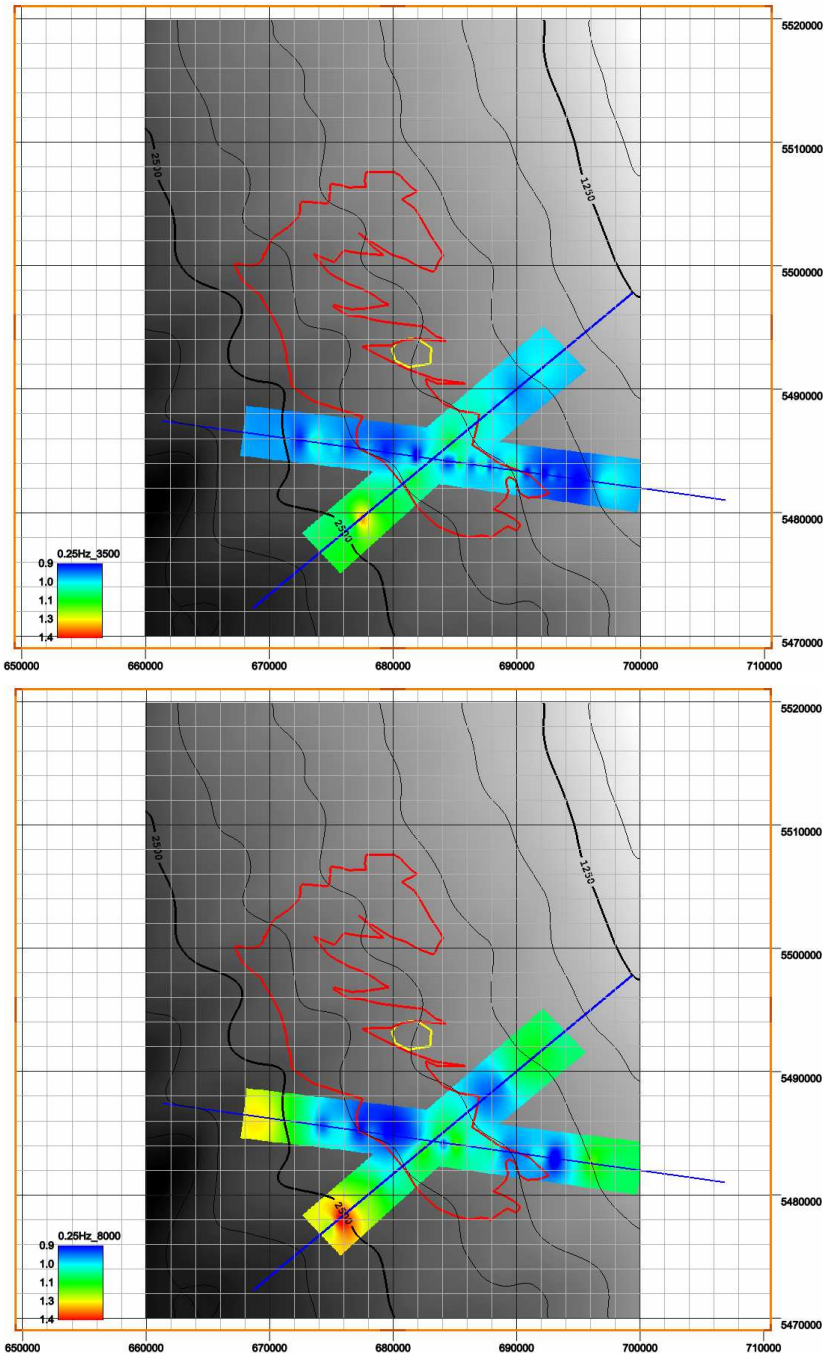

Figure 7-3 *Wolseley area responses superimposed on a seabed depth map - normalized electric magnitudes for 1st harmonic (0.25 Hz) at ± 3.5 km (upper) and ± 8.0 km (lower). Strength of the normalized anomalies is indicated by the colour bar to the left.*

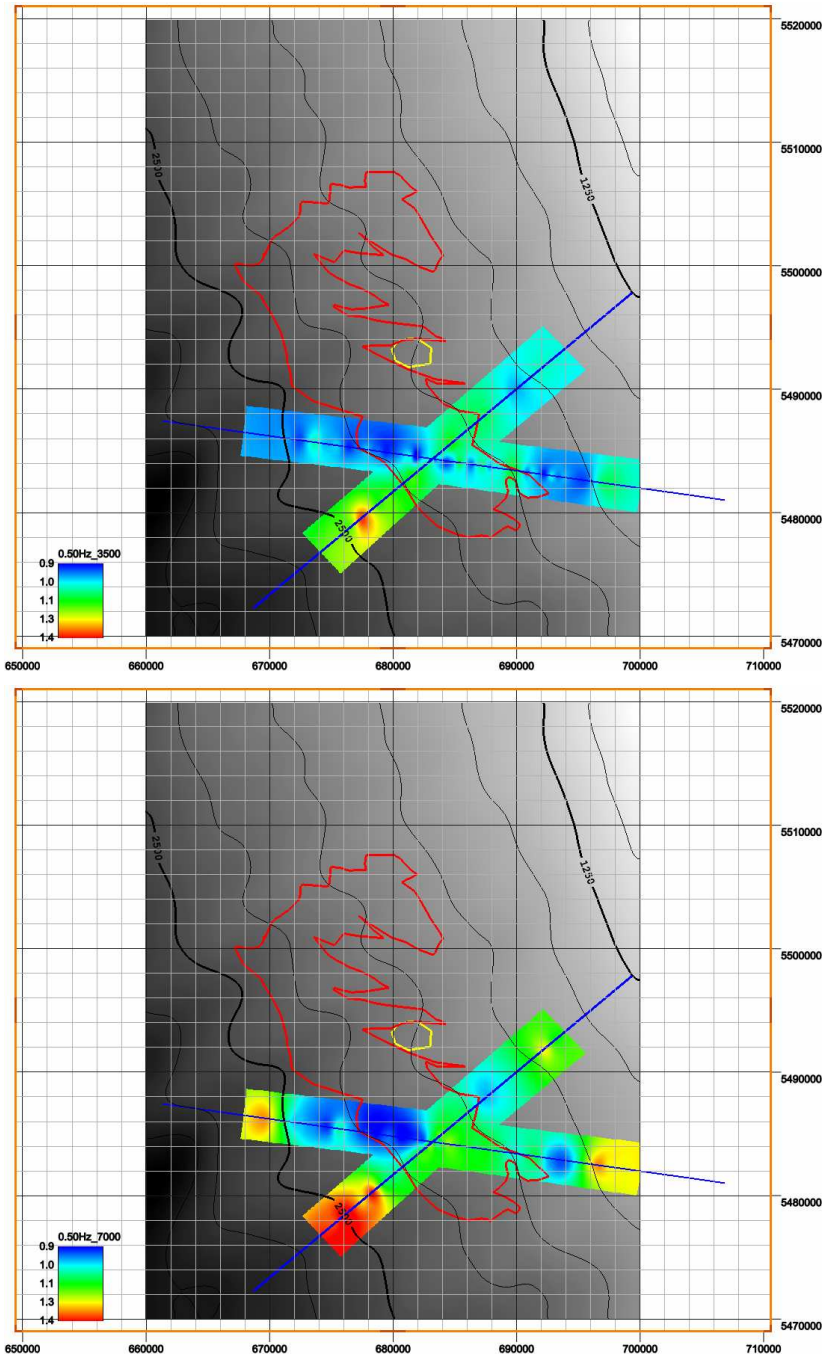

Figure 7-4 *Wolseley area responses superimposed on a seabed depth map - normalized electric magnitudes for 2nd harmonic (0.50 Hz) at ± 3.5 km (upper) and ± 7.0 km (lower). Strength of the normalized anomalies is indicated by the colour bar to the left.*

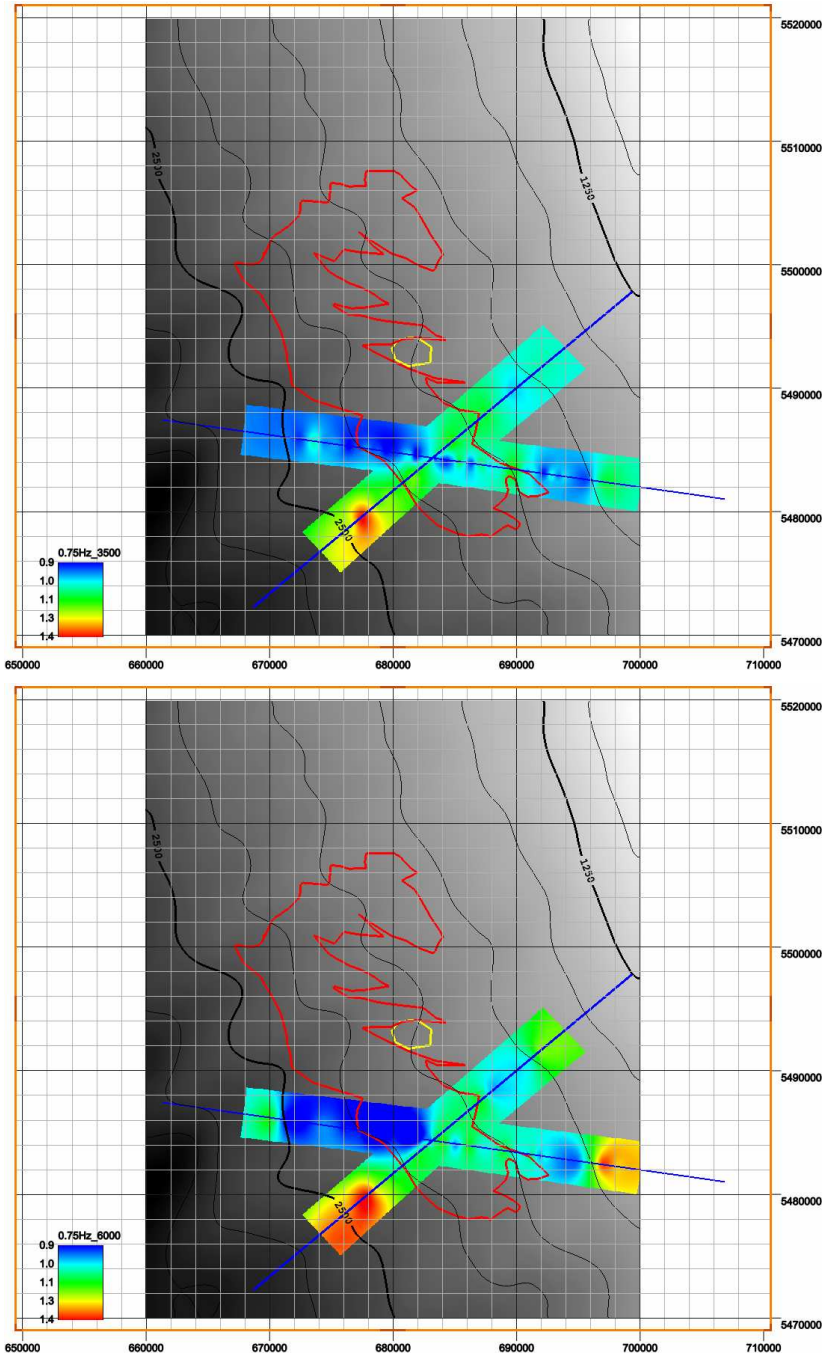

Figure 7-5 *Wolseley area responses superimposed on seabed depth map - normalized electric magnitudes for 3rd harmonic (0.75 Hz) at ± 3.5 km (upper) and ± 6.0 km (lower). Strength of the normalized anomalies is indicated by the colour bar to the left.*

7.3 Line response

7.3.1 Standard processing

Standard processed Wolseley line responses for electric field at 1st, 2nd and 3rd harmonics and selected offsets are shown in Figure 7-6 to Figure 7-11. Two offsets were selected for each frequency. The maximum offset selected decreases with increasing frequencies.

Only electric data is presented in summary plots due to the quality at far offsets.

A weak anomaly of approximately 1.1 appears at short offset for the three frequencies 0.25Hz, 0.50Hz & 0.75Hz for both lines. However, at far offsets, anomalies are open towards both ends for the two lines.

Generally, the response is higher in strength at both ends for the two lines. In the prospect outline area, only few receivers show weak response at very near to the crossing point.

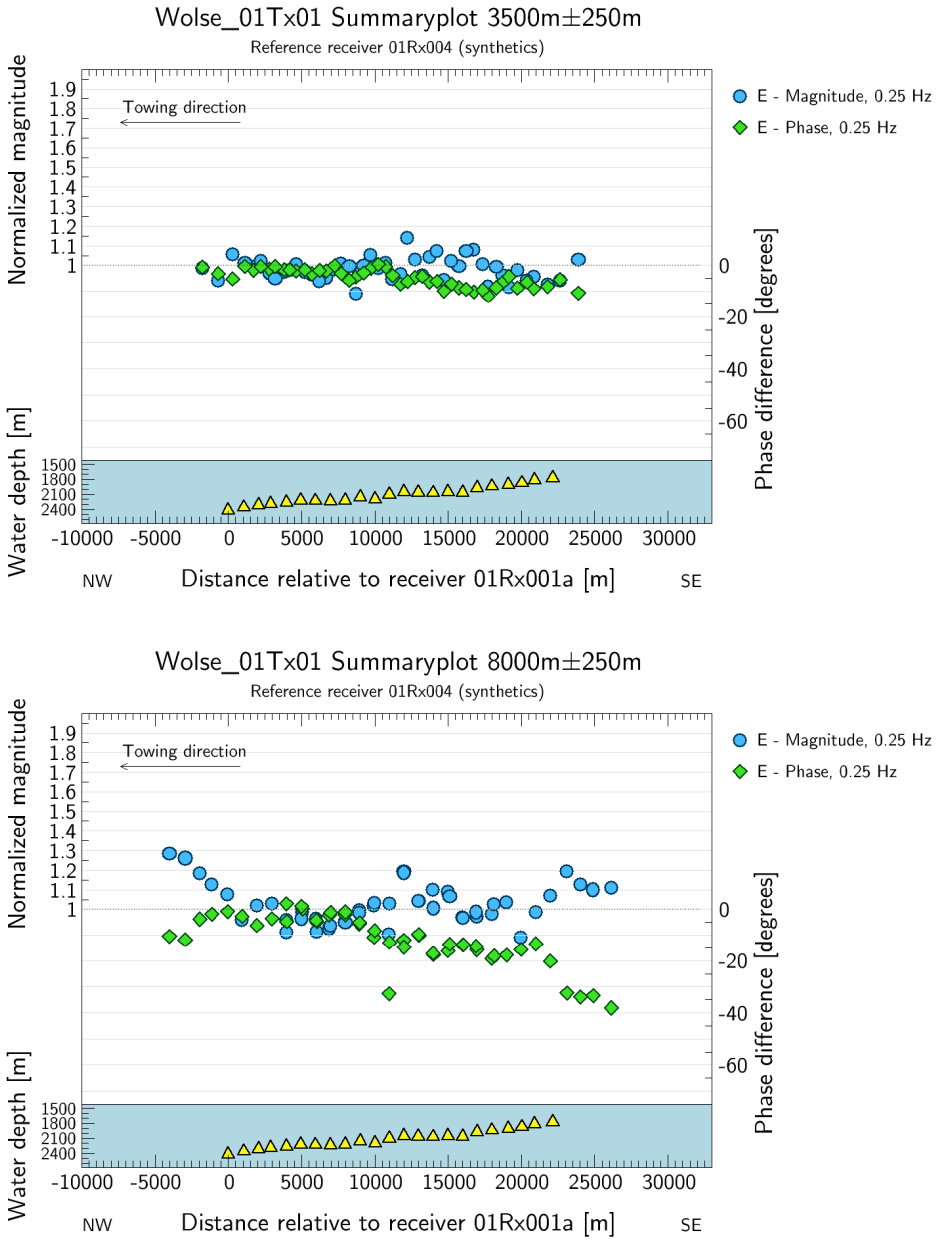

Figure 7-6 ***Wolse01Tx01*** *line response at 1st harmonic (0.25 Hz) – electric normalized magnitude and phase difference at ± 3.5 km (upper) and ± 8.0 km (lower). The lower parts of the figures show receiver positions and water depth along the transmitter line.*

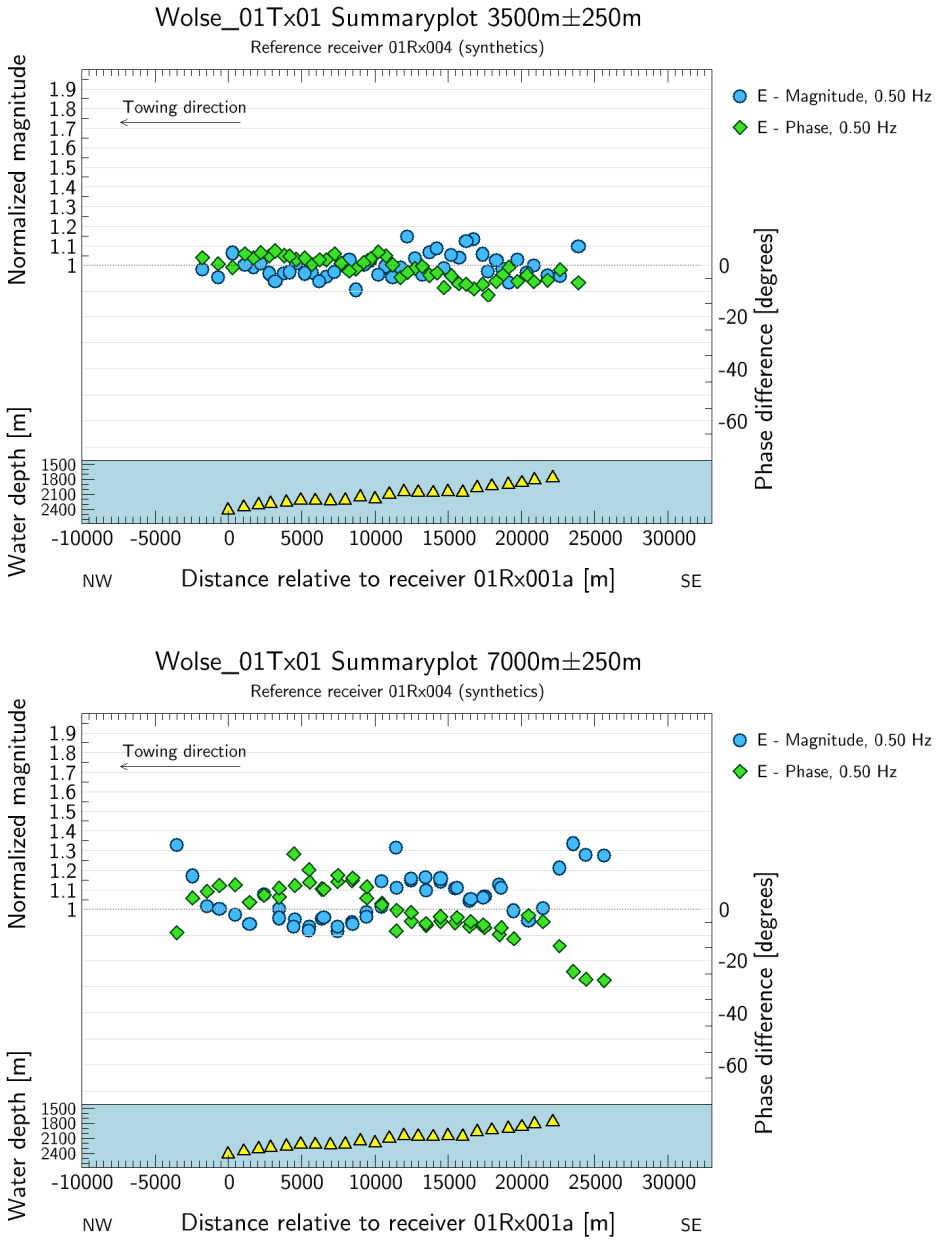

Figure 7-7 ***Wolse01Tx01*** *line response at 2nd harmonic (0.50 Hz) – electric normalized magnitude and phase difference at ± 3.5 km (upper) and ± 7.0 km (lower). The lower parts of the figures show receiver positions and water depth along the transmitter line.*

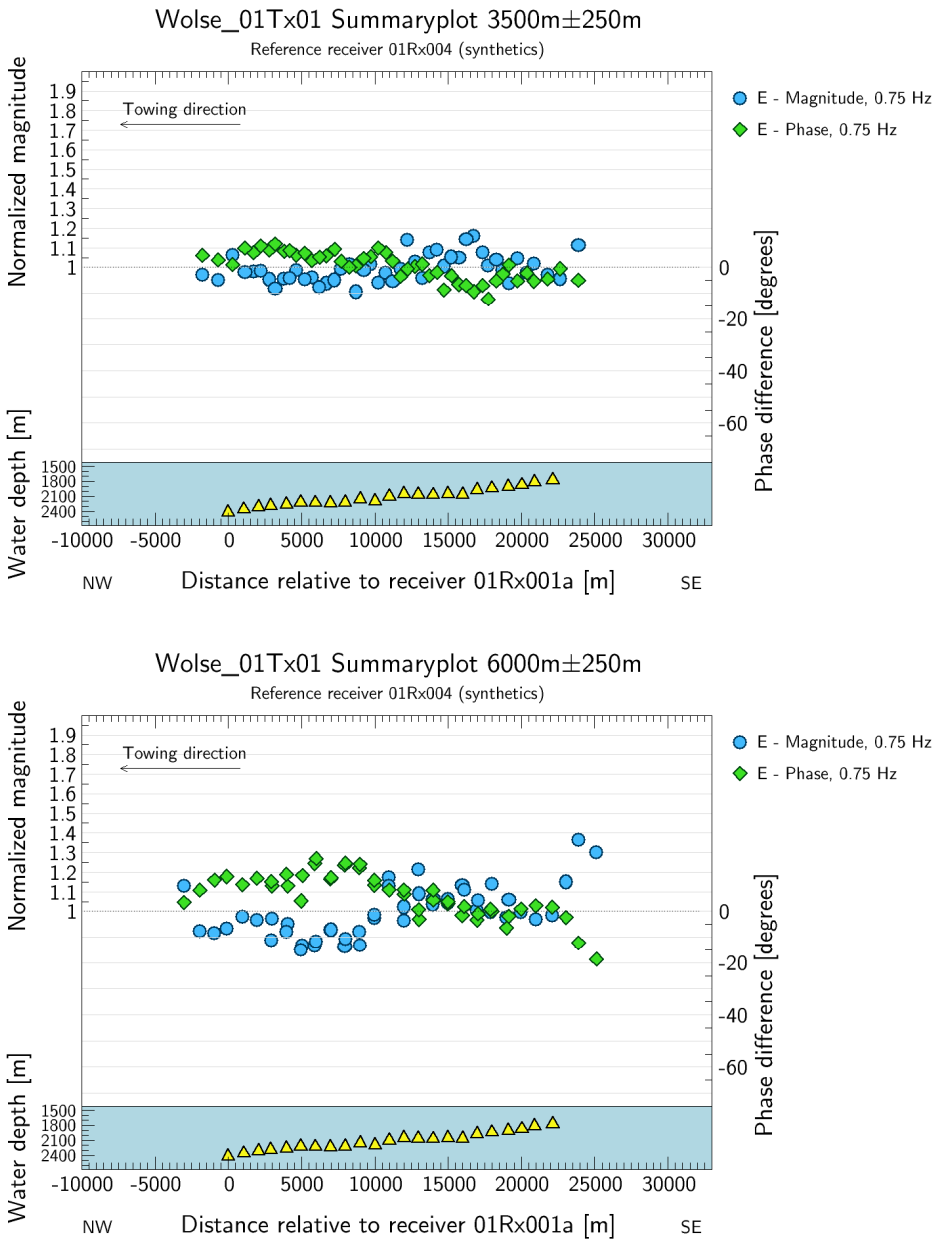

Figure 7-8 ***Wolse01Tx01*** *line response at 3rd harmonic (0.75 Hz) – electric normalized magnitude and phase difference at ± 3.5 km (upper) and ± 6.0 km (lower). The lower parts of the figures show receiver positions and water depth along the transmitter line.*

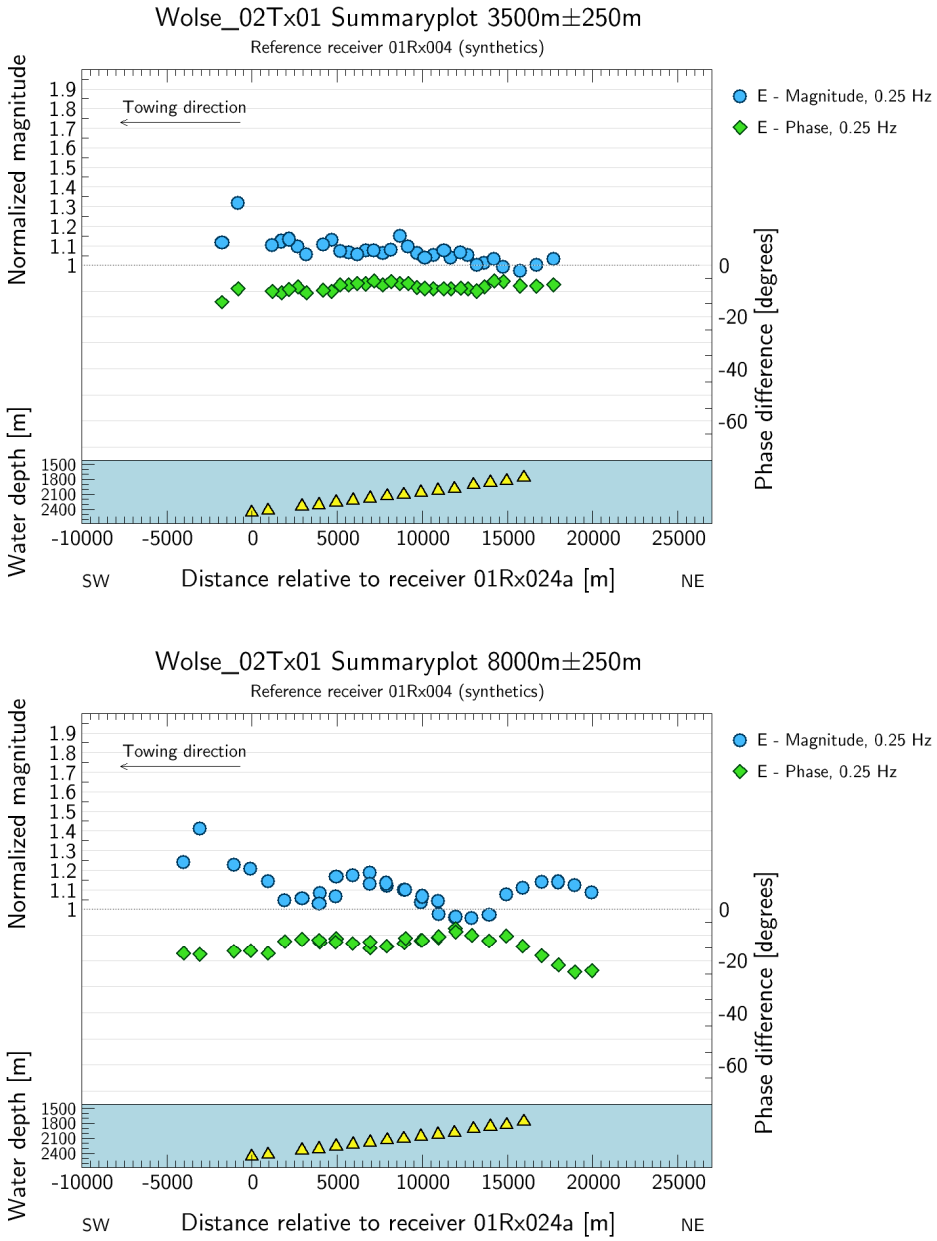

Figure 7-9 ***Wolse02Tx01*** *line response at 1st harmonic (0.25 Hz) – electric normalized magnitude and phase difference at ± 3.5 km (upper) and ± 8.0 km (lower). The lower parts of the figures show receiver positions and water depth along the transmitter line.*

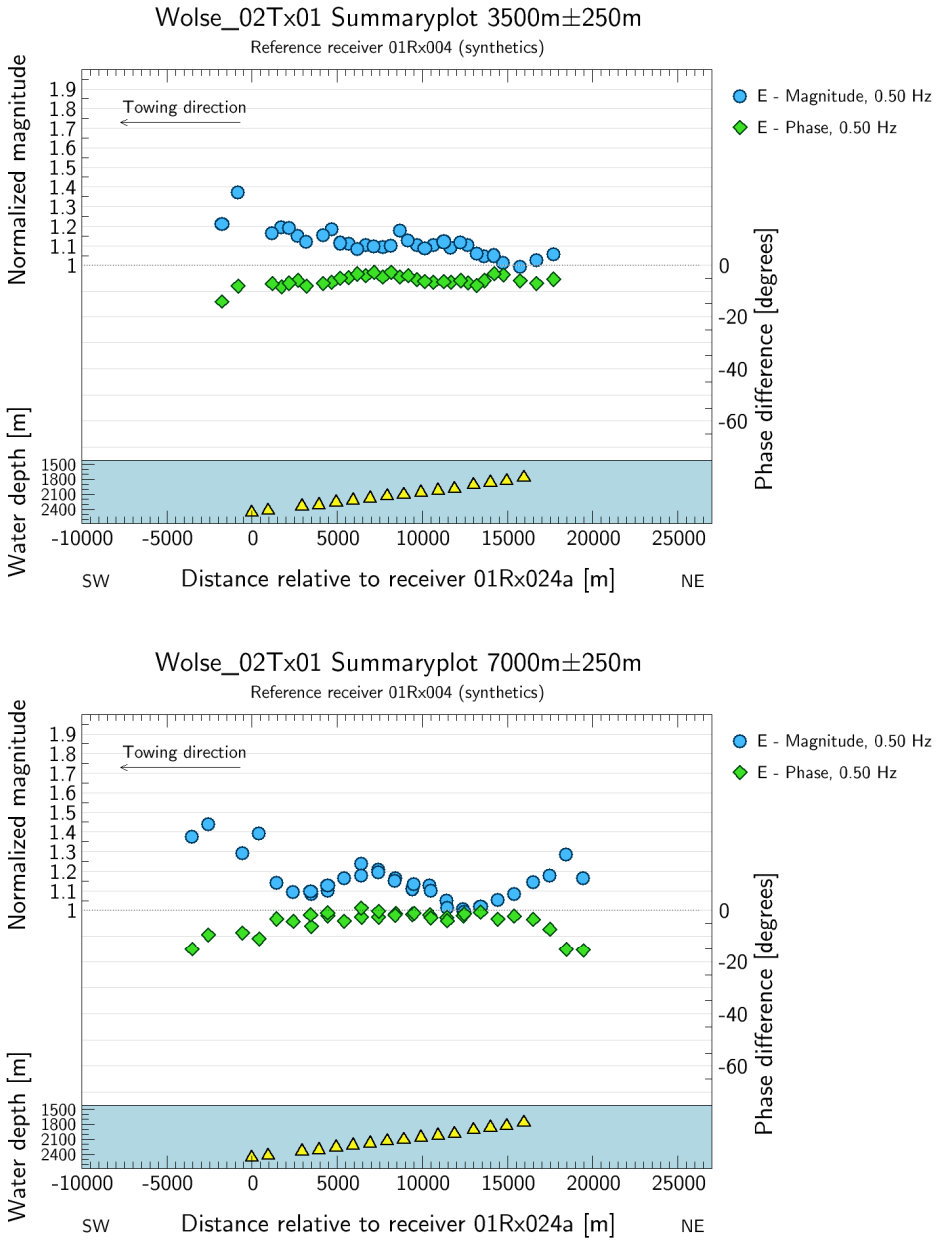

Figure 7-10 ***Wolse02Tx01*** *line response at 2nd harmonic (0.50 Hz) – electric normalized magnitude and phase difference at ± 3.5 km (upper) and ± 7.0 km (lower). The lower parts of the figures show receiver positions and water depth along the transmitter line.*

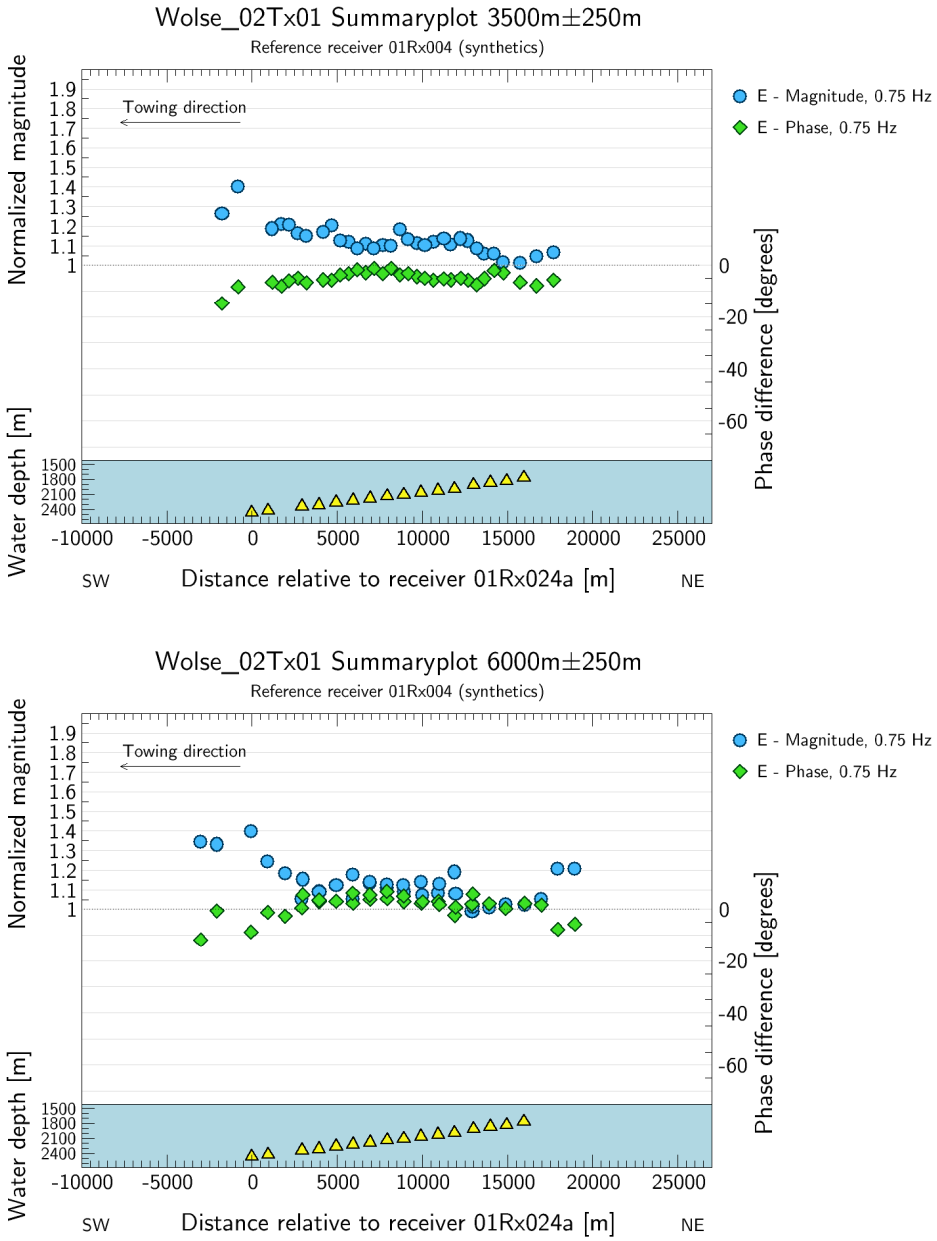

Figure 7-11 ***Wolse02Tx01*** *line response at 3rd harmonic (0.75 Hz) – electric normalized magnitude and phase difference at ± 3.5 km (upper) and ± 6.0 km (lower). The lower parts of the figures show receiver positions and water depth along the transmitter line.*

7.4 Receiver responses

Responses recorded by the following receivers are presented in this section:

01Rx006 on Wolse01Tx01
01Rx017 on Wolse01Tx01
01Rx028 on Wolse02Tx01
01Rx035 on Wolse02Tx01

Locations of these receivers are shown in Figure 7-12

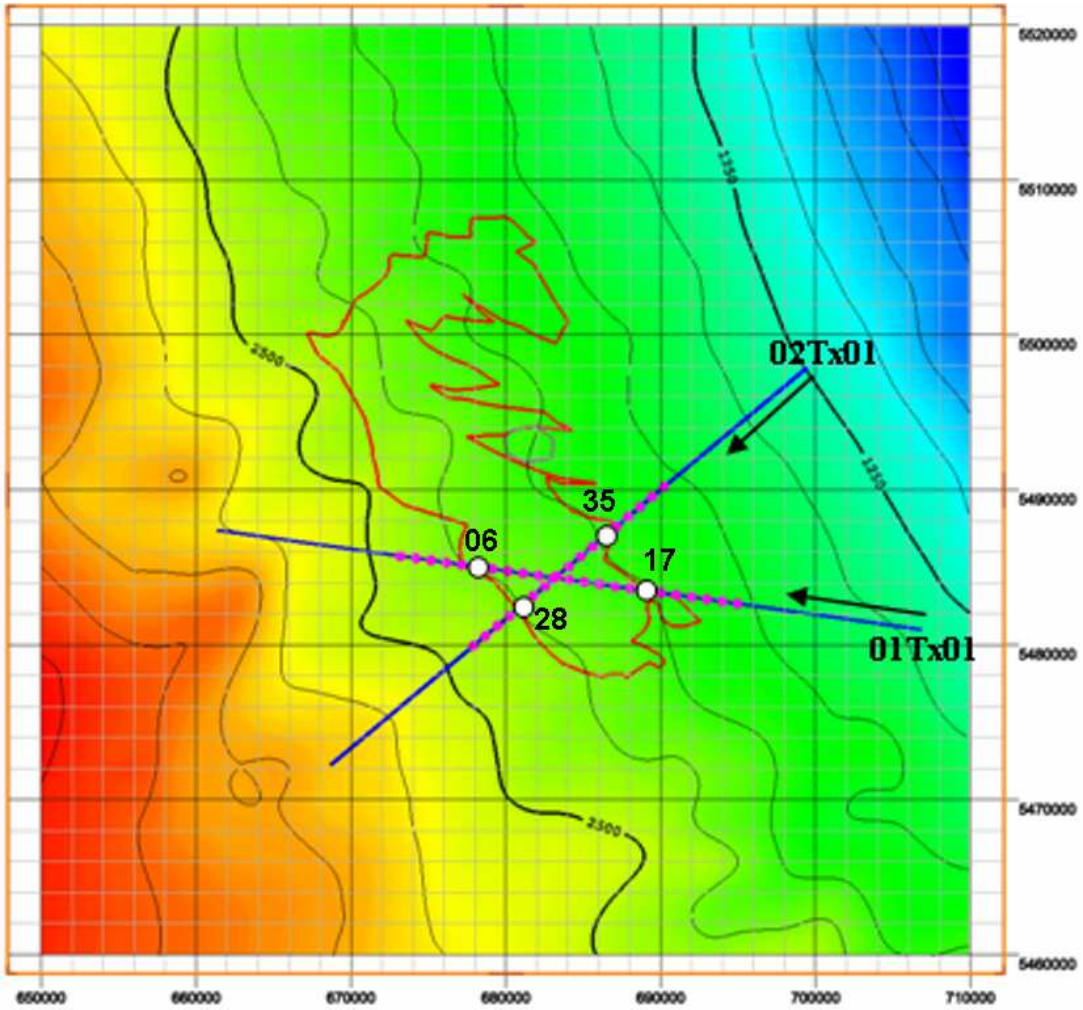

Figure 7-12 *Survey layout map with receiver positions and transmitter lines. Receivers 01Rx006, 01Rx017 01Rx028 and 01Rx035 are labelled and shown as circles with white fill.*

7.4.1 Standard processing

Standard processed normalized electric/magnetic magnitude and electric/magnetic phase responses are shown in Figure 7-13 to Figure 7-16 for receiver 01Rx006 and 01Rx017 along Wolse01Tx01 and receiver 01Rx028 and 01Rx035 along Wolse02Tx01 at the three main frequencies (0.25 Hz, 0.50 Hz and 0.75 Hz). At high frequencies, influence of noise can be observed at shorter offsets.

Receiver 01Rx006 along towline Wolse01Tx01 shows weak normalized electric / magnetic responses of approximately below 1 at short to intermediate offsets. The responses are increasing in strength at far offsets.

Receiver 01Rx017 along towline Wolse01Tx01 shows a weak response. However, the normalized electric data show slightly higher out-towing response than in-towing. The responses are increasing in strength at far offsets.

Receiver 01Rx028 along towline Wolse02Tx01 shows a weak response of slightly above 1. The normalized electric / magnetic data show slightly higher out-towing responses than in-towing. It is observed that normalized electric response is slightly higher than magnetic.

Receiver 01Rx035 along Wolse02Tx01 shows a weak response. The normalized electric / magnetic data show slightly higher out-towing response than in-towing. The responses are increasing in strength at far offsets.

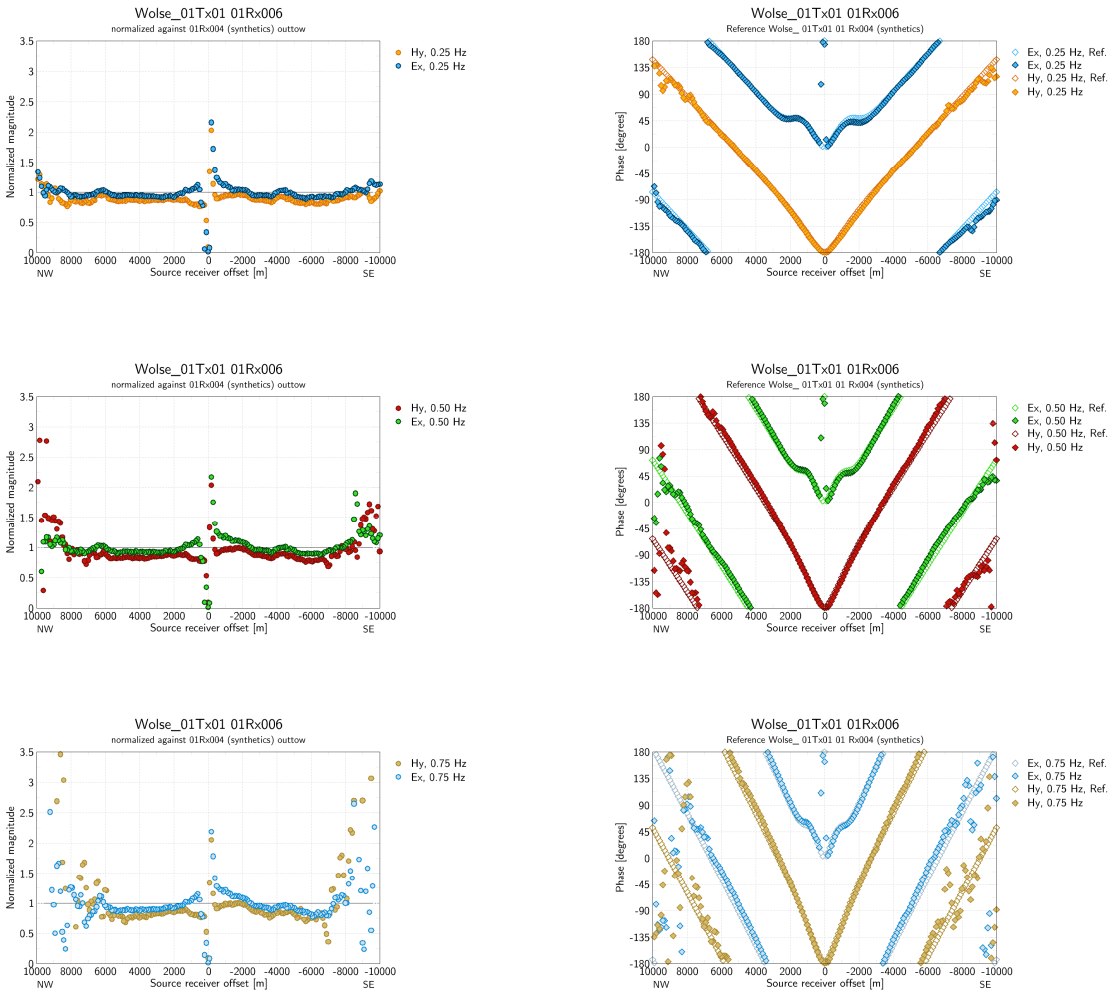

Figure 7-13 *Standard processing – 01Rx006 along Wolse01Tx01: Normalized electric/magnetic magnitude (left) and electric/magnetic phase comparison towards the reference receiver (right). Frequencies are 0.25 Hz (top), 0.50 Hz (middle) and 0.75 Hz (bottom).*

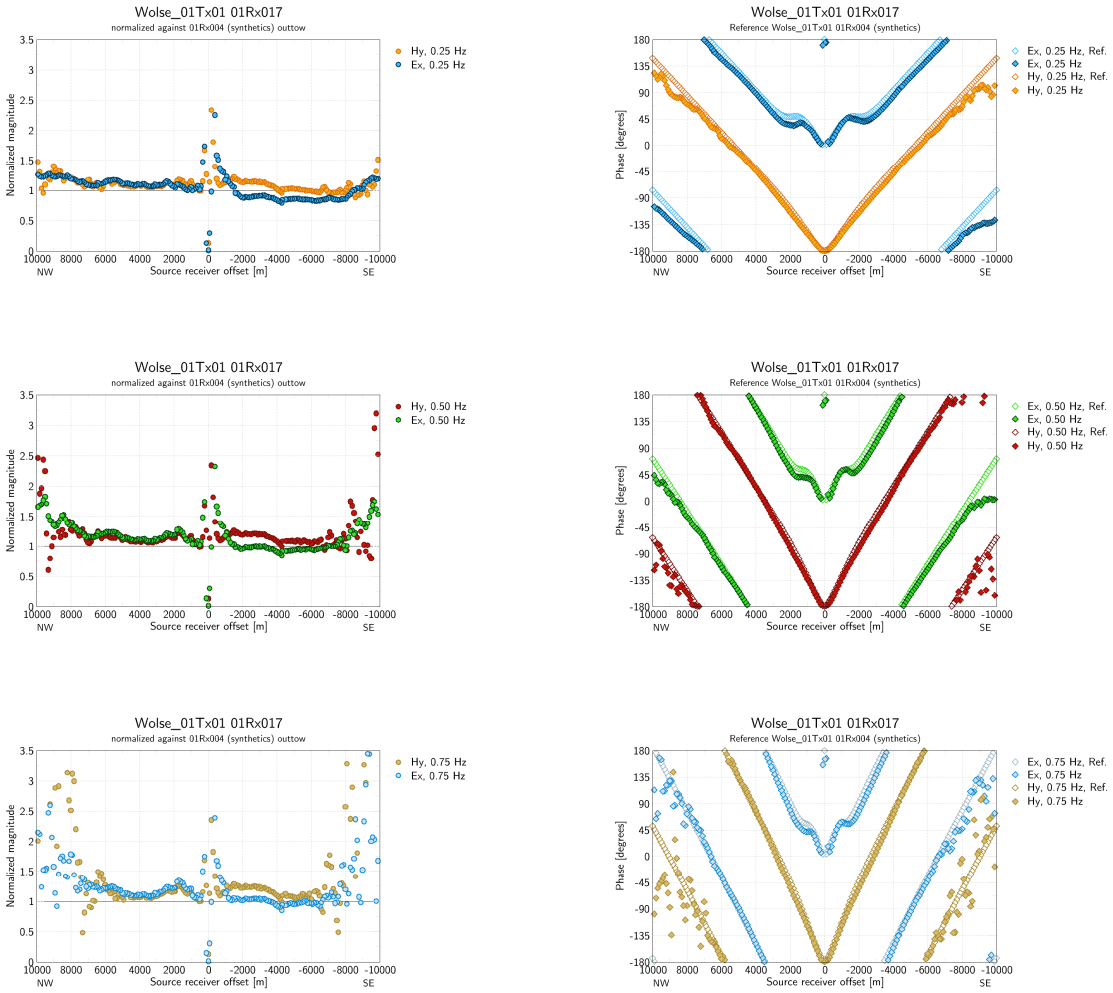

Figure 7-14 *Standard processing – 01Rx017 along Wolse01Tx01: Normalized electric/magnetic magnitude (left) and electric/magnetic phase comparison towards the reference receiver (right). Frequencies are 0.25 Hz (top), 0.50 Hz (middle) and 0.75 Hz (bottom).*

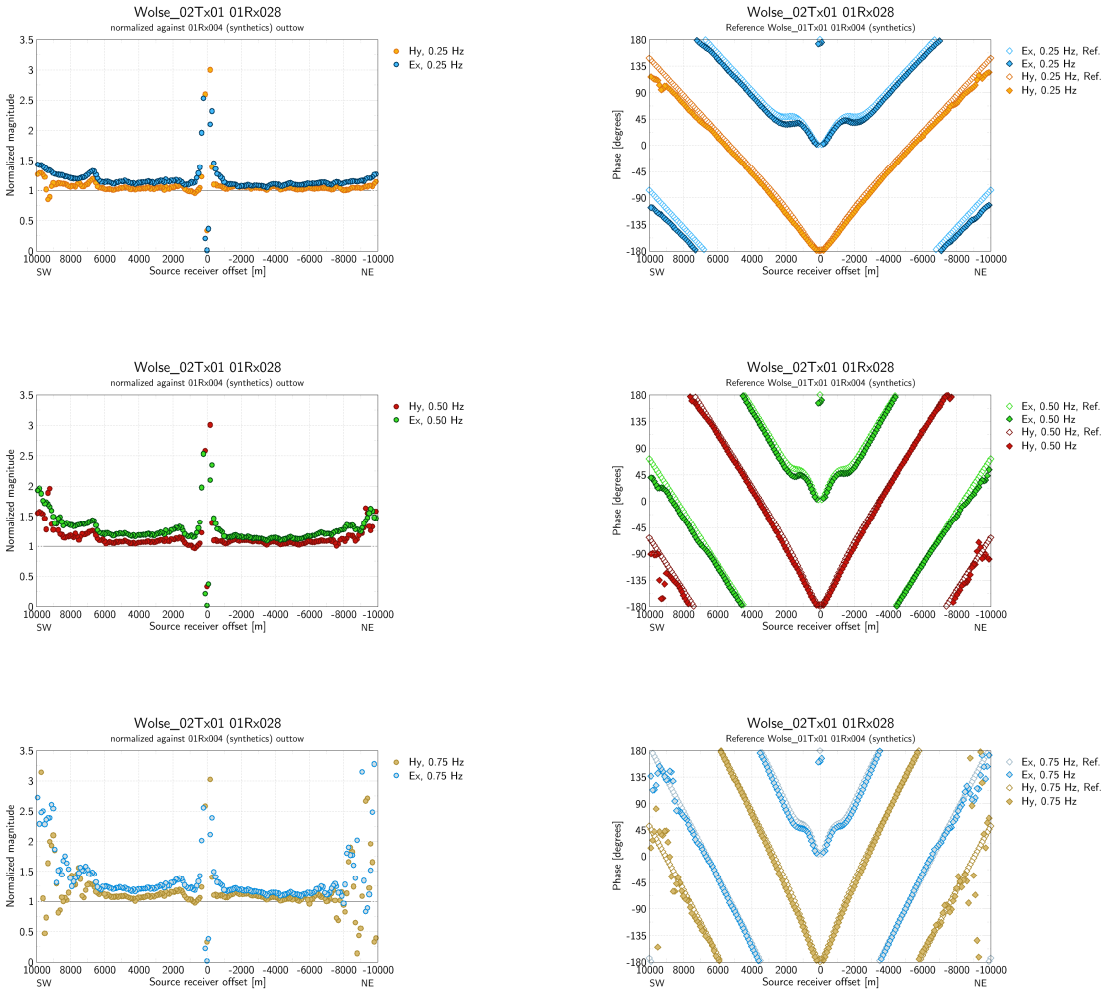

Figure 7-15 *Standard processing – 01Rx028 along Wolse01Tx01: Normalized electric/magnetic magnitude (left) and electric/magnetic phase comparison towards the reference receiver (right). Frequencies are 0.25 Hz (top), 0.50 Hz (middle) and 0.75 Hz (bottom).*

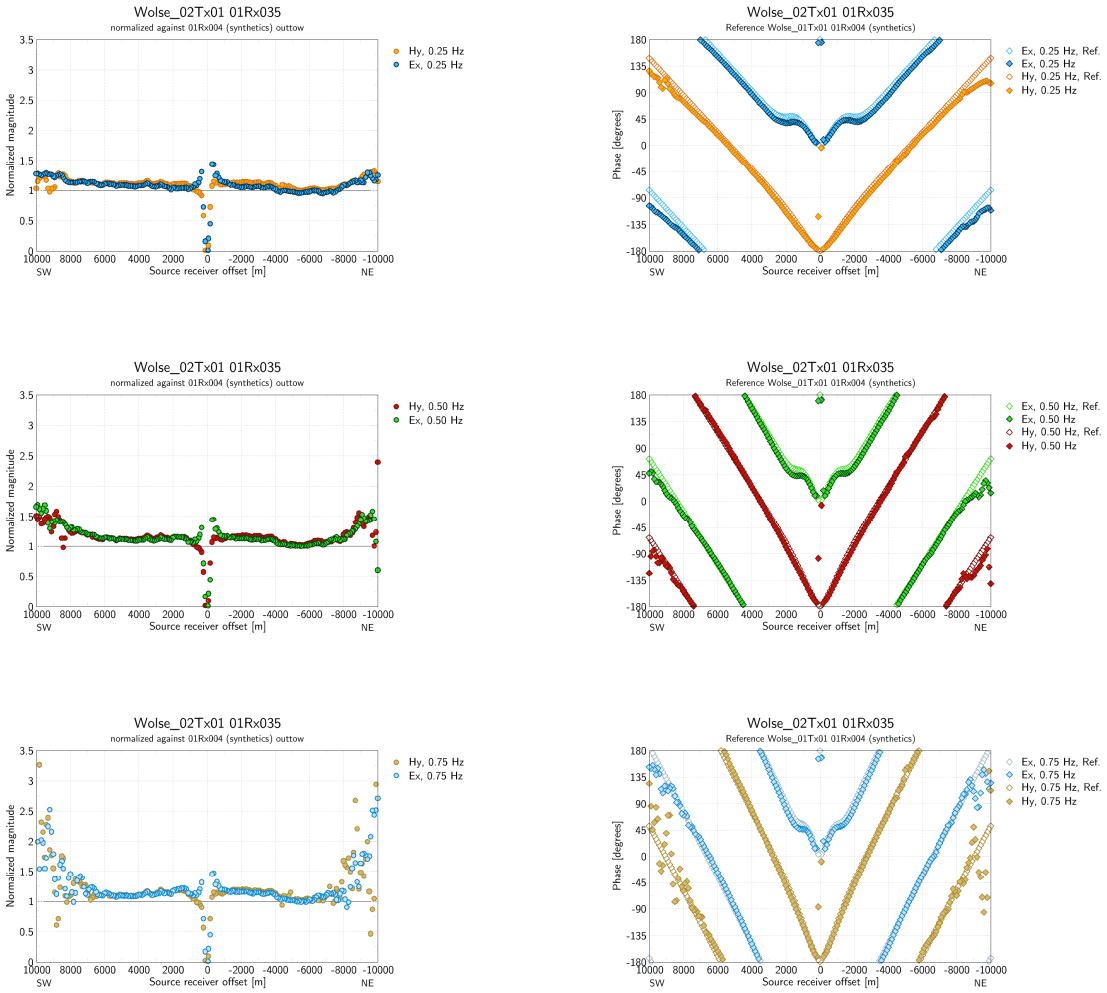

Figure 7-16 *Standard processing – 02Rx035 along Wolse02Tx01: Normalized electric/magnetic magnitude (left) and electric/magnetic phase comparison towards the reference receiver (right). Frequencies are 0.25 Hz (top), 0.50 Hz (middle) and 0.75 Hz (bottom).*

8 Summary

A SeaBed Logging (SBL) survey was performed in Sorell Basin, Australia. The data was acquired in August 2007. A total of 44 receivers were deployed along two lines. All receivers measured both the electric and magnetic field in two orthogonal directions (Ex, Ey, Hx and Hy) with redundant measurements for the electric field. Water depth in the survey area varies from 1700 to 2500 meters.

High quality electric data was recorded up to 8-10 km at 0.25 Hz (base frequency), 8-9 km at 0.50 Hz (second harmonic) and 6.5-7.5 km at 0.75 Hz (third harmonic). The quality of the electric field measurement is slightly higher than the magnetic field measurement. Due to the large water depth in the survey area, no up-down separation of standard processed signals was performed.

At short offsets, weak anomalies are observed close to the crossing point of Wolse01Tx01 and Wolse02Tx01. At large offsets, weak to moderate anomalies are open at both ends for the two lines. Anomalies are indicated by a positive normalized magnitude and negative phase difference. At higher frequencies, noise influences at shorter offsets.

Further analysis should be carried up to understand and explain the data

9 References

Øvstedal, M., Huse, T.H., & Berntsen, M., 2007: “Data acquisition report, Wolseley” emgs report.